Coordination Chemistry Reviews 255 (2011) 1342–1359

Contents lists available at ScienceDirect

Coordination Chemistry Reviews

journal homepage: www.elsevier.com/locate/ccr

Review

Reactivity of white phosphorus with compounds of the *p*-block☆

Nick A. Giffin, Jason D. Masuda*

The Maritimes Center for Green Chemistry and the Department of Chemistry, Saint Mary's University, Halifax, NS, B3H 3C3, Canada

Contents

ARTICLE INFO

Article history:
Received 23 September 2010
Accepted 16 December 2010
Available online 8 January 2011

Keywords:
White phosphorus
Elemental phosphorus
Phosphorus compounds
Synthesis
Main-group chemistry
Small molecule activation

ABSTRACT

This review covers the activation, aggregation and degradation of white phosphorus by molecules containing reactive *p*-block centers. The chemistry has been divided into a number of reaction types and possible mechanisms are used to aid in the understanding of these reactions.

1. Introduction and history

The history of phosphorus originates in the quest for the Philosopher's Stone. It is generally agreed that Hennig Brandt can be credited with the discovery and naming of elemental phosphorus in 1669 [1]. His fascination with the Philosopher's Stone and the mind-set of the time, that the source could be derived from human body, lead Brandt to follow an elaborate recipe [1]. When broken down into a simple chemical reaction, this process involved the heating of human urine to ultimately yield an impure mixture of $NaPO_3$ and carbon which

Abbreviations: Ar^{Dipp}, 2,6-bis(2,6-di-*iso*-propylphenyl)phenyl; CAAC, cyclic alkyl amino carbene; Ch, chalcogen; cHex, cyclohexyl; Cp*, pentamethylcyclopentadienyl; Dipp, 2,6-di-*iso*-propylphenyl; DMP, 2,6-bis(2,4,6-tri-methylphenyl)-phenyl; Mes, mesityl; Mes*, 2,4,6-tri-*tert*-butylphenyl; Nacnac, [Dipp]NC-(Me)CHC(Me)N[Dipp]$^-$; NHC, *N*-heterocyclic carbene; THF, tetrahydrofuran.

☆ During the preparation of this manuscript, three reviews on the chemistry of white phosphorus were published. These include P_4 activation by early transition metals by Cummins et al. [148], P_4 activation using late transition metals by Peruzzini et al. [149] and main group activation of P_4 by Scheer et al. [150]. It is hoped that this review will complement these other works and stimulate continued research in the chemistry of white phosphorus.

* Corresponding author. Tel.: +1 902 420 5077; fax: +1 902 496 8104.
E-mail address: jason.masuda@smu.ca (J.D. Masuda).

0010-8545/$ – see front matter © 2011 Elsevier B.V. All rights reserved.
doi:10.1016/j.ccr.2010.12.016

then would react at high temperatures to give $2Na_4P_2O_7 + 10CO + P_4$.

Most chemists are familiar with the painting by Joseph Wright of Derby *The Alchymist Discovering Phosphorus* (1771) [2,3]. It is believed to depict Brandt's discovery of the element as well as its striking chemiluminescent properties when white phosphorus is exposed to trace amounts of oxygen. This dramatic (for its time) effect is attributed to PO_2 which is derived from the following reaction: $O + PO \rightarrow PO_2^*$ [4]. Due to its chemiluminescent properties, the element was named after the ancient Greek word for the planet Venus, the morning star or bringer of light [5].

Currently, white phosphorus is made by reacting calcium phosphate, sand and coke in an electric arc furnace at over 1473 K and is separated by cooling and collecting gaseous P_4.

$$2Ca_3(PO_4)_2 + 6SiO_2 + 10C \rightarrow 6CaSiO_3 + P_4 + 10CO$$

Worldwide production of white phosphorus has dropped dramatically primarily as a result of more efficient hydrometallurgic processes that have replaced the production of phosphates for use in agriculture and low-grade phosphoric acid [6]. In contrast, most P(III) and P(V) compounds that contain a phosphorus–carbon bond are still made through the laborious halogenation of P_4 with chlorine to give PCl_3, which is then reacted with alkyl or aryl metal salts (typically group 1 or group 2 metals) to form the new P–C bond. Although there has been a steady state of synthetic inorganic research using white phosphorus, recently there has been a resurgence of interest including investigations towards the catalytic derivatization of P_4 to useful molecules. This interest is partially encompassed in the increasingly stringent environmental and transportation regulations regarding P_4 as well as avoiding chlorine-based syntheses.

There have been a number of reviews discussing the chemistry of white phosphorus. The coordination chemistry of P_4 and its activation products has been reviewed by Scherer [7–9], followed by two reviews by Peruzzini et al. in 2002[10] and 2005 [11]. The extensive work by Baudler on polyphosphorus and polyphosphide compounds, which often involved P_4 chemistry, has also been reviewed [12,13]. A number of reviews focused on the organic or main group chemistry of elemental phosphorus are available [14–18]. The most recent [18], by Milyukov et al., published in 2005, outlined the formation of organophosphorus compounds by a number of routes, including electrochemical methods. Furthermore, the topic of electrochemical/electrocatalytic formation of organophosphorus compounds has recently been discussed a number of times by Budnikova et al. [19–21]. The present review will mainly focus on the *p*-block chemistry of white phosphorus since 2005, with particular attention on the possible types of reactivity that may occur. It is the intention of the authors that this focus will assist those new to the field and aid in the collective understanding of the diverse reactivity exhibited by white phosphorus.

2. Allotropes of phosphorus

White phosphorus is the most notable allotrope of elemental phosphorus in terms of reactivity as well as application within munitions and incendiary manufacturing. Occupying a tetrahedral cage geometry in the crystalline state, white phosphorus is the least stable and most reactive allotrope of elemental phosphorus that persists under ambient conditions [1,22]. Thermal, γ-ray and photo-degradation of P_4 to the red or black allotropes is thermodynamically favored and P_4 has been observed to be in an equilibrated state with its dissociated P_2 fragment when approaching 1070 K. Free P_2 has been defined as 49 kcal/mol higher in energy than neutral P_4 and has yet to be observed at room temperature [23–27]. The P–P bond lengths in the P_4 tetrahedron have been studied

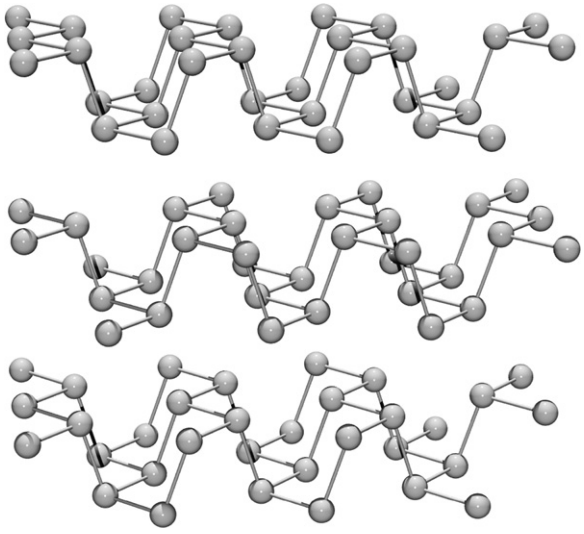

Fig. 2.1. Solid state structure of black phosphorus [39].

rigorously and have yet to show strong agreement in value [28]. Quantum mechanical calculations show a P–P length of 2.194 Å [29] however Raman spectroscopy (2.2228(5) Å) [30] and electron diffraction techniques (2.21 Å at 470 K) [31] have yielded variable results. At room temperature white phosphorus exists in the α-form. At 196 K a reversible transition from α-P_4 to β-P_4 occurs, a structure which has been characterized using single crystal X-ray diffraction with an observed P–P bond distance of 2.209(5) Å [32,33]. When α-P_4 is quenched to 88 K a transition to the γ-P_4 conformation has been observed and characterized using X-ray powder diffraction [34]. Interestingly, γ-P_4 transitions to β-P_4 at 153 K however, to this date a β to γ transformation has not been reported [32,33].

The reactivity of white phosphorus can be mediated by the formation of inclusion or intercalating complexes. Using the stabilizing arene interactions of fullerenes, Green et al. produced a $(P_4)_2C_{60}$ repeating unit, representing the first reported case of host–guest white phosphorus chemistry [35]. As an extension of this principal, Nitschke et al. have reported a self-assembly mechanism for white phosphorus encapsulation. The iron (II) based capsule may then be used as a stable source of P_4 through the addition of a competing host to the tetrahedral container [36]. Recently Cummins et al. have reported on the properties and reactivity of the P_4 analogue As_3P, indicating other tetrahedral mixed pnictogen species may be viable [37].

Following X-ray powder diffraction work by Hultgren et al. in 1935 [38], Brown and Rundqvist isolated crystalline black phosphorus using a growth medium of liquid bismuth [39]. Analysis using single crystal X-ray diffraction indicated a graphite-like layering of puckered 6-membered rings. This densest and least reactive allotrope of phosphorus has both pressure induced and temperature dependent phase transitions to rhombohedral semimetallic as well as cubic metallic phases [40–42], and is a semi-conducting material [43] (Fig. 2.1).

In comparison to the white and black allotropes, the definition of red phosphorus is less complete. Obtained through thermal, ultraviolet or γ-ray degradative polymerization of white phosphorus, the red allotrope has been proposed to exist in five unambiguous forms [28,44,45]. Type I is commercially available amorphous red phosphorus through which Types II–V may be generated *via* high temperature annealing. Calculations by Haser et al. describing the relative energies of various phosphorus allotropes propose that Type I is a combination of fibrous red and Hittorf's phosphorus, Types IV/V respectively, along with a P_{12} helical structure later

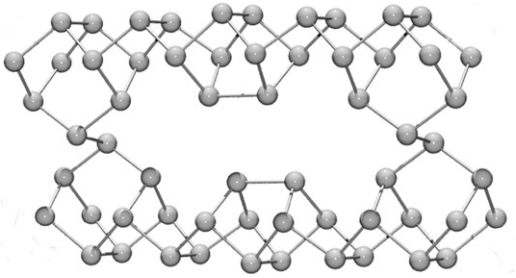

Fig. 2.2. Single crystal structure of fibrous red phosphorus [49].

characterized by work in CuI matrices [29,46–48]. Structural data regarding Types II–III has not been obtained and are at present ill-defined. In 2005, Type IV was structurally identified though single crystal X-ray crystallography by Ruck et al. [49]. Characterized as fibrous red phosphorus, the most recent addition to the phosphorus family exists as a polymeric structure of linked pentagonal rings (Fig. 2.2).

Type V is the branched violet form known as Hittorf's phosphorus, a tribute to Hittorf who first described it in 1865 [50]. Although definitive structural characterization was not completed until 1969 by Thurn and Krebs using single crystal X-ray crystallography, this branched form of elemental phosphorus has been nominally attributed to its cardinal observer [51,52] (Fig. 2.3).

The asymmetric unit of both Hittorf's and fibrous red phosphorus includes a repeating unit of 21 single phosphorus atoms. From the X-ray crystallographic data of the fibrous red allotrope it was proposed that the arrangement of the phosphorus atoms is similar to that in Hittorf's phosphorus with the exception of the branches, which are instead oriented in a parallel manner [49]. Type IV red phosphorus was considered to be energetically stable by Ruck et al. while Böcker and Haser have since concluded that Hittorf's and fibrous red phosphorus are energetically equivalent and the most stable of all the characterized red phosphorus conformations to date [29].

The existence of various polymeric forms of red phosphorus of similar stability is proposed by Boecker and Haeser [53]. The theoretical studies on these energetically analogous polymeric units have been supported experimentally by the repeating phosphorus units found in CuI based matrices. $(CuI)_3P_{12}$ [46], $(CuI)_8P_{12}$ [54] and $(CuI)_2P_{14}$ [55] structures have been observed to date, through which nanorod-like materials may be formed through removal of CuI by a KCN solution [47]. Described as nanowires and nanorods, silicon wafer supported optical microscopy and scanning electron microscopy has elucidated structural details of these red phosphorus strands, and is supported by energy-dispersive X-ray spectroscopy. Transmission electron microscopy (TEM) indicates that these materials are polycrystalline structures with lattice spacing on the order of 5.7 Å. High resolution TEM relates the structural properties of these phosphorus nanorods to those of Type II red phosphorus with additional distinct characteristics. Nanomaterials of elemental phosphorus have also been produced *via* polymerization of P_4 with bismuth nanoparticles to give a proposed red phosphorus structure [56]. In addition, ^{60}Co radiation of P_4 in benzene forms a nanocomposite P_n material [57].

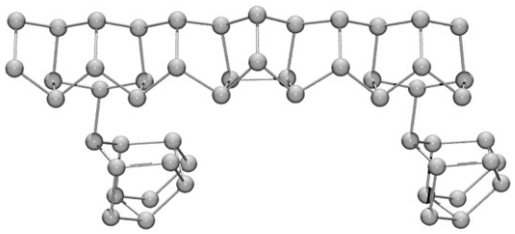

Fig. 2.3. Single crystal structure of Hittorf's (violet) phosphorus [51,52].

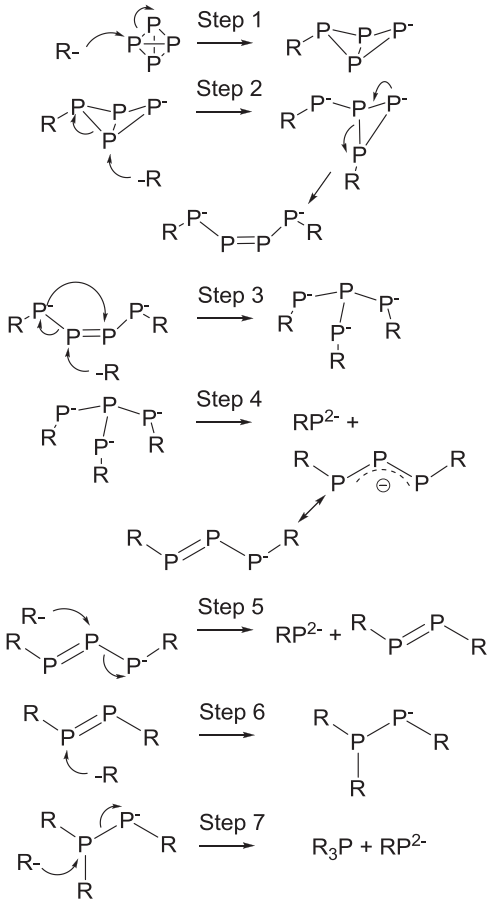

Scheme 3.1. Possible multi-step mechanism for the activation and subsequent degradation of white phosphorus by a nucleophilic species.

Neutral phosphorus clusters of various sizes and connectivity have been studied theoretically to elucidate potential energetically viable closed shell clusters. High order computational analysis on neutral P_n phosphorus clusters where $n = 4$ [58,59], 6 [60–67], 8 [25,68–71] as well as ionic $[P_n]^x$ clusters collectively outline the energetic relationship among the proposed structures [66,72–80]. Both the aromatic P_6 cyclohexaphospha-benzene and anionic cyclo-P_5 have been studied computationally and have been utilized as ligands in synthetic chemistry [81–86]. More comprehensive comparison based reports on structures ranging from P_2 to P_{28} have been completed [24,29,53,87–91] and extend in the literature to icosahedral and ring systems in the P_n mold ($n = 80$, 180, 320, 500, 720) [92].

3. Reactions with *p*-block nucleophiles

The nucleophilic attack of white phosphorus by *p*-block elements has historically been one of the more commonly investigated methods of white phosphorus derivatization. This is, of course, due to the extensive usage of organoalkali and organoalkali earth reagents in synthetic chemistry. The reactivity of nucleophiles typically follows the steps outlined below (Scheme 3.1): Step 1, nucleophilic attack at the P_4 tetrahedron resulting in the breakage of one P–P bond to give the monosubstituted anionic tetraphosphabicyclo[1.1.0]butane; Step 2, nucleophilic attack at one of the bridgehead phosphorus atoms, followed by a rearrangement gives the 1,4-disubstituted tetraphosphenediide. This species can then

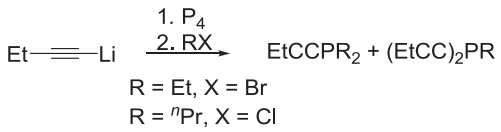

Scheme 3.1.1. Formation of acetylene substituted tertiary phosphines from white phosphorus.

go on to Step 3 or dimerize *via* a [2 + 2] cycloaddition through the P=P double bond; Step 3, attack at one of the central phosphorus atoms, followed by rearrangement gives the $[(RP)_3P]^{3-}$ ion; Step 4, degradation of the original P_4 fragment through loss of RP^{2-} to give the triphosphide $[R_2P_3]^-$; Step 5, Nucleophilic attack at the central phosphorus atom followed by loss of RP^{2-} gives the diphosphene. This species can then go on to Step 6 or oligomerize to form molecules of the form $(RP)_n$; Step 6, attack at one of the phosphorus atoms gives the diphosphide $[R_2P–P(R)]^-$; Step 7, nucleophilic attack at the neutral phosphorus atoms results in the formation of the tertiary phosphine and diphosphide.

3.1. Group 14

Classic examples of nucleophilic attack of white phosphorus with Group 14 anions include the formation of primary and secondary phosphines in very low yields from lithium or Grignard reagents containing phenyl or *n*-butyl groups [93]. Although the exact composition of the reaction intermediates are not known, it was noted that upon quenching reaction mixtures with water, no PH_3 was produced. This indicated that M_3P is not present in the reaction mixtures but rather polyphenylphosphides are most likely present. These results are in line with the proposed mechanisms in Scheme 3.1 for the nucleophilic activation and degradation of white phosphorus. Similar reactions of aryl lithium reagents with white phosphorus and *n*-butyl halides gave mixtures of products that primarily consist of diarylbutyl phosphines or aryldibutyl phosphines [94]. In the same study, tetra(*n*-butyl)cyclotetraphosphine $(^nBuP)_4$, was prepared in 42% yield by the reaction of *n*-butyl lithium with *n*-butyl bromide and 0.5 equiv. P_4. More recently, it was shown that the reaction of lithium butynide with P_4 and quenching with ethyl bromide or *n*-propyl chloride gave mixtures of the tertiary phosphines in ca. 10% yields (Scheme 3.1.1) [95].

Nucleophilic attack of P_4 with CN^- results in the formation of two products, namely [18-crown-6-K][$P(CN)_2$] and [18-crown-6-K][P_{15}]. Similar products are formed when tetraethyl- and tetrabutylammonium cations are used [96]. Although the products of the reaction do not necessarily fit the mechanisms outlined in Scheme 3.1, they are most likely the result of disproportionation resulting in the aggregation P_n fragments to form the P_{15} anion.

Utilizing the sterically demanding Mes* (2,4,6-tri-*tert*-butylphenyl) group, Fluck et al. used the combination of addition of Mes* lithium with white phosphorus and quenching with Mes* bromide to isolate both the diphosphene, Mes*-P = P-Mes* and the tetraphosphabicyclo[1.1.0]butane, Mes*-P_4-Mes* (Scheme 3.1.2) [97]. This example was the first reported case where only one bond of the P_4 tetrahedron is broken. The single crystal structure

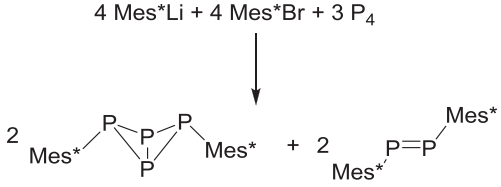

Scheme 3.1.2. Formation of tetraphosphabicyclo[1.1.0]butane and diphosphene from a one-pot reaction containing aryl lithium, aryl bromide and white phosphorus.

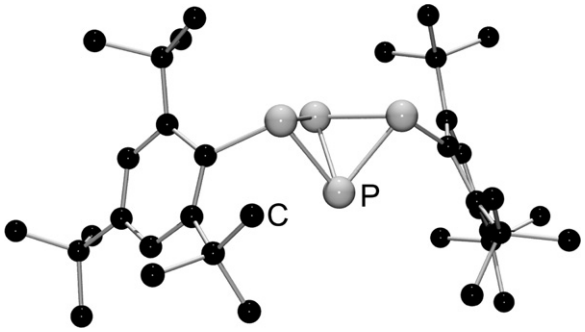

Fig. 3.1.1. Solid state structure of bis(2,4,6-tri-*tert*-butylphenyl) tetraphosphabicyclo[1.1.0]butane [97]. Hydrogen atoms have been removed for clarity.

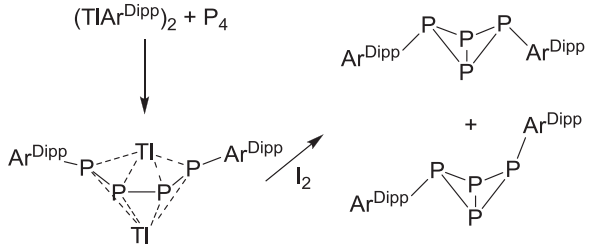

Scheme 3.1.3. Formation of tetraphosphabutadienediide and iodine oxidation to the tetraphosphabicyclo[1.1.0]butane.

confirmed the formation of the tetraphosphabicyclo[1.1.0]butane (Fig. 3.1.1).

Nucleophilic attack by the bulky terphenyl thallium reagent $(TlAr^{Dipp})_2$ ($Ar^{Dipp} = C_6H_3$–2,6-(C_6H_3–2,6-$^iPr_2$)$_2$) with white phosphorus gives the tetraphosphabutadienediide capped by two Ar^{Dipp} groups with the thallium cations each coordinating above or below the P–P–P–P chain in an η^4-fashion (see Scheme 3.1.3 and Fig. 3.1.2) [98]. The formation of this species follows Steps 1 and 2 in Scheme 3.1. Analysis of the bond lengths from the solid state structure reveals that the system behaves as if the 2^- charge is delocalized through the $[Ar^{Dipp}–P–P–P–P–Ar^{Dipp}]^{2-}$ chain giving a P–P bond order of 1.33 rather than localized with separate charges on the outer P-atoms and a central P=P double bond as described by $Ar^{Dipp}–P^-–P=P–P^-–Ar^{Dipp}$. The interaction with the thallium atoms may give rise to this delocalization. Oxi-

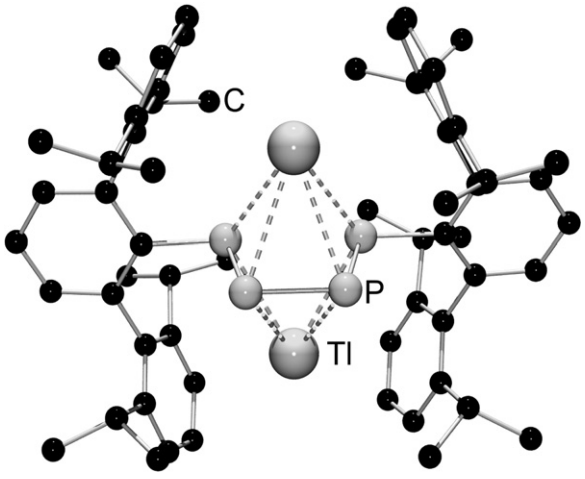

Fig. 3.1.2. Solid state structure of thallium coordinated tetraphosphabutadienediide $Tl_2[P_4\{C_6H_3$-2,6-$(Dipp)_2\}]$ [98]. Hydrogen atoms have been removed for clarity.

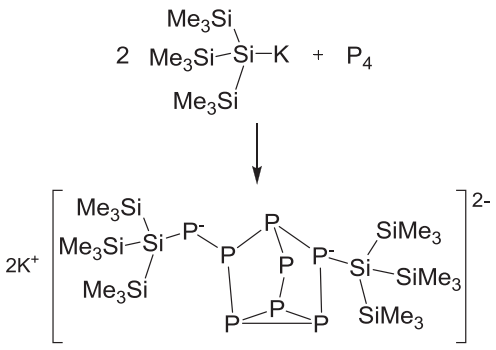

Scheme 3.1.4. Formation of $[\{(Me_3Si)_3Si\}_2P_8]^{2-}$.

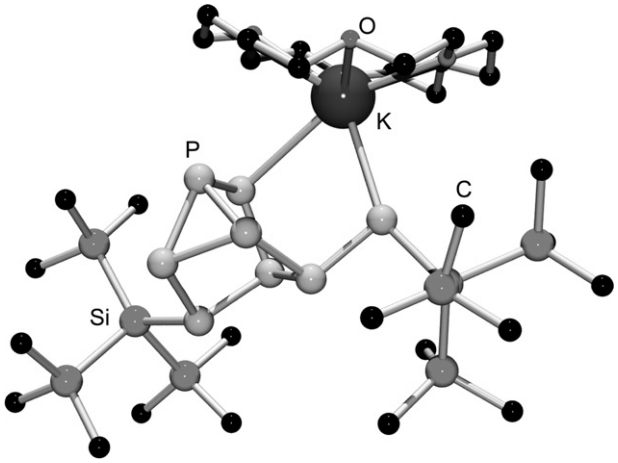

Fig. 3.1.3. Solid state structure of the polycyclic octaphosphadiide complex [(18-crown-6)K][P_8(Si{$SiMe_3$}$_3$)] [99]. Hydrogen atoms and one non-coordinated K(18-Crown-6)$_2$ fragment have been omitted for clarity.

dation of the tetraphosphabutadienediide with elemental iodine gives the tetraphosphabicyclo[1.1.0]butane. It is interesting to note that when crystallized from benzene, the tetraphosphabicyclo[1.1.0]butane crystallizes in the *trans*,*trans* configuration whereas when crystals are grown from hexane, the *cis*,*trans* isomer is isolated.

Sterically bulky silanides have been used to isolate a number of products that can be considered as intermediates in the nucleophilic degradation pathway of white phosphorus. For example, in the 1:1 reaction of the extremely bulky potassium tris(trimethylsilyl)silylide with white phosphorus, the formation of the dianion $[\{(Me_3Si)_3Si\}_2P_8]^{2-}$ occurs (Scheme 3.1.4 and Fig. 3.1.3) [99]. It was proposed that P_8 species forms *via* dimerization of two

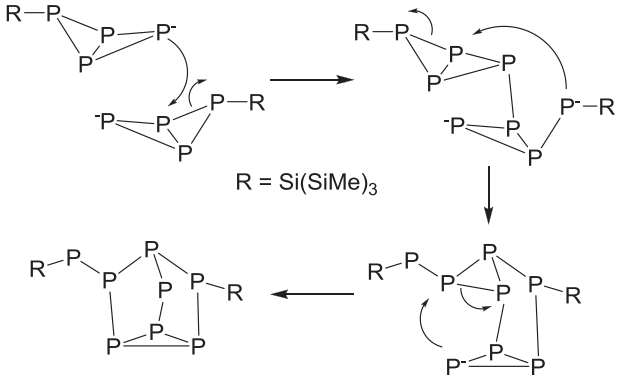

Scheme 3.1.5. Proposed mechanism for the formation of P_8-dianion.

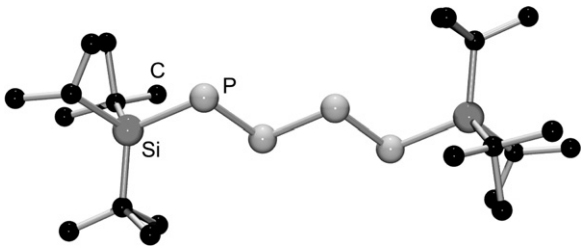

Fig. 3.1.4. Solid state structure of tetraphosphadiide $[(^tBu_3SiP)_2P_2]^{2-}$ [100]. Hydrogen atoms and the non-coordinated 18-Crown-6 and Na(18-Crown-6)(THF)$_2$ fragments have been omitted for clarity.

RP_4^- fragments (Scheme 3.1.5) which would be formed *via* Step 1 in Scheme 3.1.

When the slightly less bulky tri-*tert*-butylsilyl group is used, a number of products from Steps 2, 3 and 4 of Scheme 3.1 are isolated (see Scheme 3.1.6). Reaction of $^tBu_3SiM$ (M = Li, Na, K) in a 2:1 ratio with white phosphorus in THF gives the tetraphosphenediide salts $M_2[^tBu_3Si\text{-}P_4\text{-}Si^tBu_3]$ (M = Li [100], Na [100,101], K [100,102]). The solid state structure of the sodium salt is shown in Fig. 3.1.4. In this case, when the reaction is run in *tert*-butyl methyl ether the tetraphosphenediide dimerizes *via* a [2 + 2] cycloaddition through the diphosphene fragments to form $Na_4[(^tBu_3SiP)_4P_4]$ (Fig. 3.1.5). Addition of THF to this species results in the cycloelimination of the tetraphosphenediide monomers. For the lithium and sodium salts, the 3:1 reaction of $^tBu_3SiM$ with P_4 results in the formation of the tetraphosphatriide $M_3[(^tBu_3SiP)_3P]$ (Fig. 3.1.6), the product of Step 3 in Scheme 3.1 [103]. Upon storage for one week at ambient temperature in THF, the tetraphosphatriide splits into the phosphadiide, $^tBu_3SiPM_2$ and the triphosphide, $M[(^tBu_3SiP)_2P]$ as seen in Step 4 of Scheme 3.1. When $^tBu_3SiK$ is reacted in a similar manner, the tetraphosphatriide is not observed but rather the phosphide, $[^tBu_3SiP]K_2$, the triphosphide, $K[(^tBu_3SiP)_2P]$, and the pentaphosphadiide, $K_2[(^tBu_3SiP)_3P_2]$ (Fig. 3.1.7) [102]. A high yielding preparation of the sodium pentaphosphadiide has also been reported [104], however this requires a multi-step, multi-solvent procedure by first reacting four equivalents of $^tBu_3SiNa$ with P_4 in THF. Initially forming $Na_2[^tBu_3Si\text{-}P_4\text{-}Si^tBu_3]$, removal of THF and

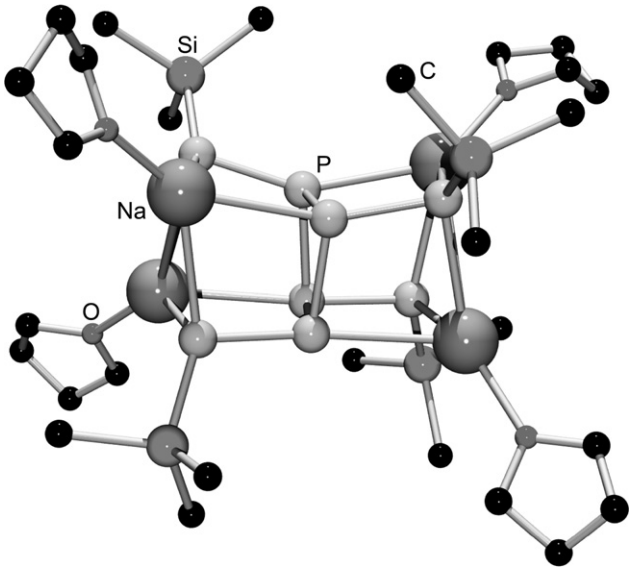

Fig. 3.1.5. Solid state structure of tetraphosphadiide [2 + 2] cycloaddition dimer $[(^tBu_3SiP)_4P_4]^{4-}$ [104]. Hydrogen atoms and methyl groups of the ^{t}Bu substituents have been omitted for clarity.

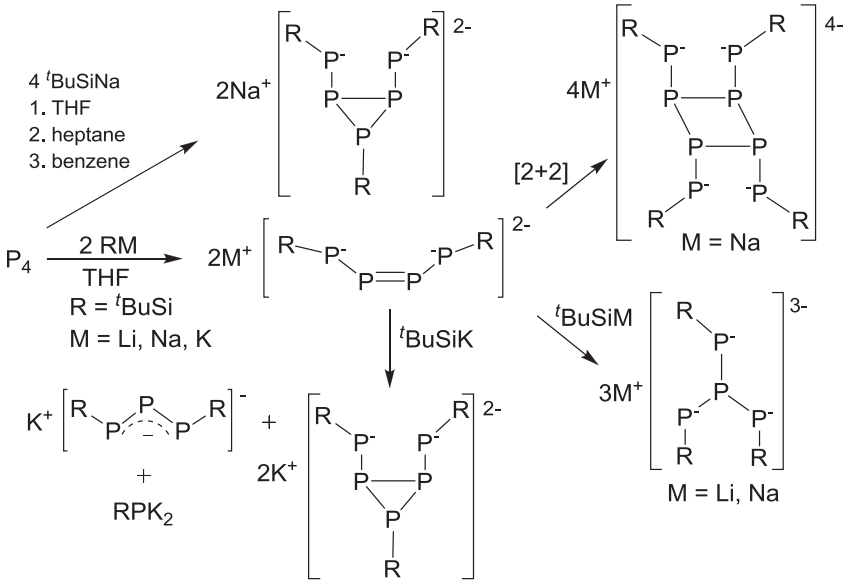

Scheme 3.1.6. Multiple outcomes for the reaction of $^{t}Bu_3SiM$ (M = Li, Na, K) with white phosphorus.

addition of heptanes yields the [2 + 2] cycloaddition product over 12 h. Finally, upon removal of heptane and stirring in benzene for 24 h at ambient temperature, formation of the final product, $Na_2[(^{t}Bu_3SiP)_3P_2]$, is observed (Fig. 3.1.8).

3.2. Group 15

The reactivity of white phosphorus with substituted alkali metal phosphides has been explored by Schmidpeter et al. [105–107]. For example, reaction of $MPPh_2$ (M = Li, Na, K) with P_4 gives the triphosphide, $[M][Ph_2P–P–PPh_2]$ and $Ph_2P–PPh_2$ as the oxidation products and M_3P_7 as reduction products. It is likely that complete fragmentation of the P_4 tetrahedron is the result of repeated nucleophilic attack by the phosphides. Other alkali metal polyphosphides and phosphinites [108] also react to give products as shown in Scheme 3.2.1.

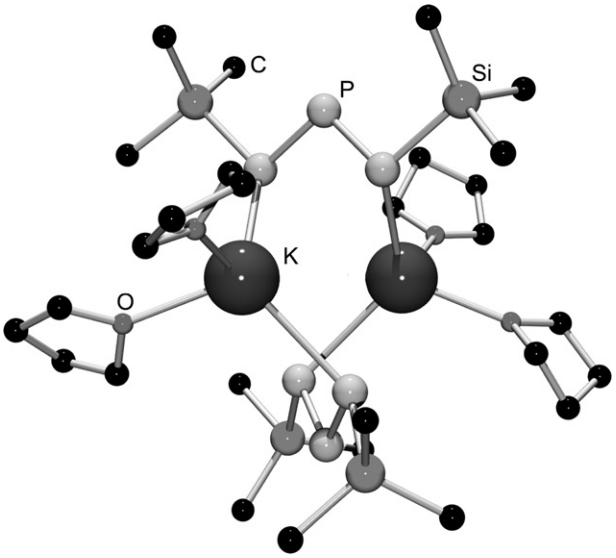

Fig. 3.1.7. Solid state structure of the potassium salt of $[(^{t}Bu_3SiP)_2P]^-$ [102]. Hydrogen atoms and methyl groups of the ^{t}Bu substituents have been omitted for clarity.

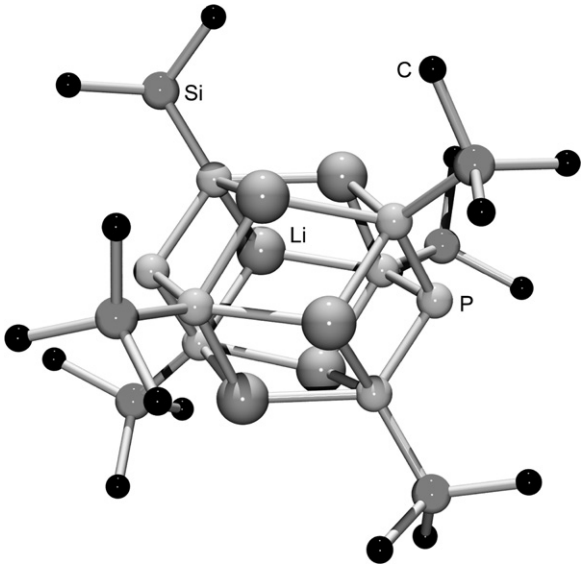

Fig. 3.1.6. Solid state structure of $Li_3[(^{t}Bu_3SiP)_3P]$ [103]. Hydrogen atoms and methyl groups of the ^{t}Bu substituents have been omitted for clarity.

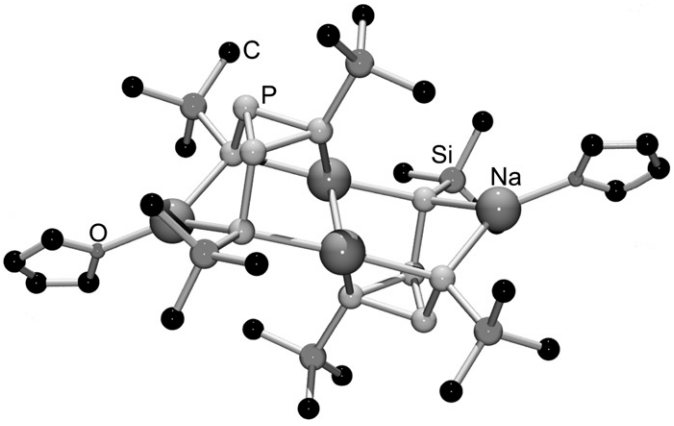

Fig. 3.1.8. Solid state structure of the sodium salt of $[(^{t}Bu_3SiP)_3P_2]^{2-}$ [104]. Hydrogen atoms and methyl groups of the ^{t}Bu substituents have been omitted for clarity.

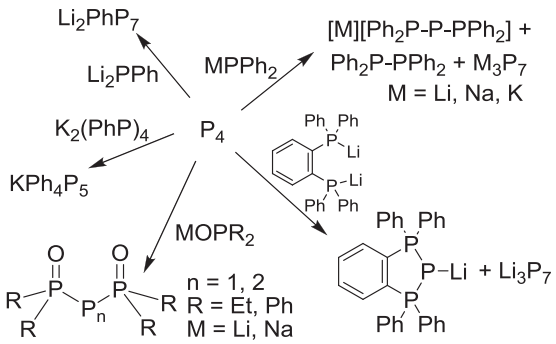

Scheme 3.2.1. Reaction of phosphorus anions with white phosphorus.

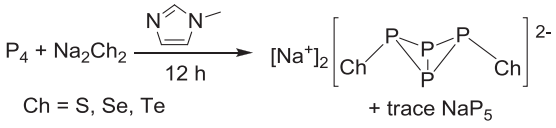

Scheme 3.3.1. Formation of chalcogen-substituted tetraphosphabicyclo[1.1.0]butanes.

3.3. Group 16

The reactivity of white phosphorus with group 16 containing species has been extensively studied [18]. Two recent studies give some insights into the nucleophilic activation and degradation of P_4. Reaction of white phosphorus with sodium dichalcogenides (Na_2Ch_2, Ch = S, Se, Te) in *N*-methyl imidazole gives the tetraphosphabicyclo[1.1.0]butane in nearly quantitative yield along with trace amounts of NaP_5 (Scheme 3.3.1) [109]. The product is the result of the Te_2^{2-} dichalcogenide insertion into a P–P bond. Phosphorus-31 NMR confirmed the structure by comparison with other tetraphosphabicyclo[1.1.0]butanes.

The reaction of P_4 with thiophenol in the presence of atmospheric oxygen and catalytic amounts of amines gave $(PhS)_3P{=}O$ in reasonable yields (Fig. 3.3.1) [110]. The authors speculate that the mechanism first proceeds *via* nucleophilic attack by PhS^- at P_4 to give the tetraphosphide (Step 1 in Scheme 3.1). The pre-activated species then reacts with diphenyldisulfide (formed through the oxidation of thiophenol in the presence of base) to give the tetraphosphabicyclo[1.1.0]butane, PhS–P_4–SPh, with elimination of PhS^-. Subsequent multiple attack by thiophenolate or diphenyldisuflide will then form $(PhS)_3P$. The fact that diphenyldisulfide plays a role in the reaction was reinforced by the formation of $(PhS)_3P{=}O$ when the amine base is replaced by catalytic amounts of diphenyldisulfide.

4. Reactions with *p*-block electrophiles

The reactivity of white phosphorus with Lewis acids of the *p*-block has been quite limited. This is most likely due to the low nucleophilicity of the P_4 molecule [22]. The sterically encumbered Group 13 molecule, Ga^tBu_3, reacts with half an equivalent of white phosphorus at room temperature to give a gallium complex chelated by two phosphorus atoms (Scheme 4.1 and Fig. 4.1) [111].

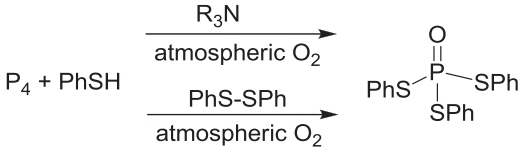

Fig. 3.3.1. Oxidative formation of *S,S,S*-triphenyl phosphorotrithiolate.

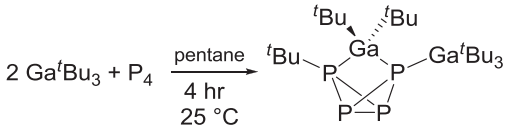

Scheme 4.1. Reaction of tri-*tert*-butyl gallium and white phosphorus.

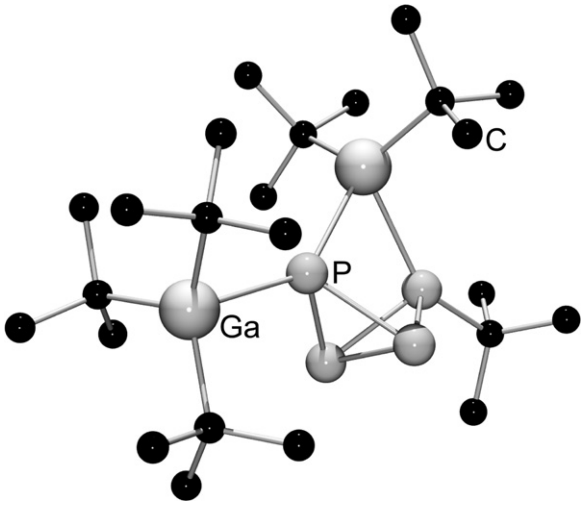

Fig. 4.1. Solid state structure of the product from the reaction of $^tBu_3Ga$ and white phosphorus [111]. Hydrogen atoms have been omitted for clarity.

It was speculated that the gallium–carbon bond added across the phosphorus–phosphorus bond of P_4. Whether a Lewis acid–base adduct is initially formed between the gallane and P_4 remains unclear.

5. Reactions with molecules containing ambiphilic centers

5.1. Overview

The activation of elemental phosphorus by main group molecules with ambiphilic character, or those that have the potential to act as Lewis acids and Lewis bases, has recently gained prevalence in the literature. The dual nature of these molecules suggests differing reaction pathways dependant on the prevailing electronic properties of the reactant in question. Based on symmetry considerations and the overall electronic structure of P_4, initiation of these events depends on the philicity of the molecule (Scheme 5.1.1). When reacting with an electrophilic molecule: (1) a P atom may donate a lone pair of electrons to a vacant *p*-orbital of an electrophile (E) forming a π-complex; (2) an electrophile may accept the electrons of a white phosphorus P–P bond, although this type of reactivity may be unfavorable due to the lack of ring strain and overall low π-character encompassed in the P–P bonds of the tetrahedron. Conversely, a nucleophilic (Nu) molecule (3) may attack an empty *p*-orbital of a phosphorus atom [112].

Generally speaking, ambiphilic activation of P_4 can be divided into two categories: in the first and most experimentally preva-

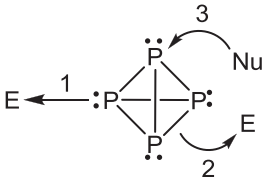

Scheme 5.1.1. Potential initiation pathways for P_4 activation [112].

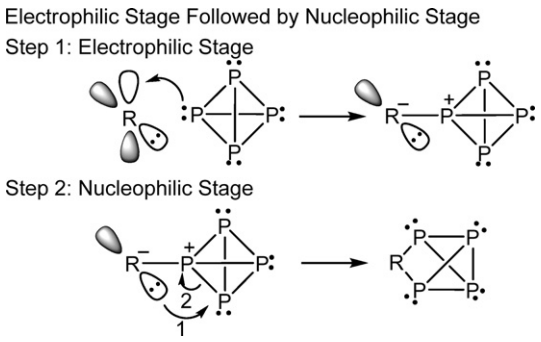

Scheme 5.1.2. Proposed mechanism for the activation of P_4 by a molecule containing a predominantly electrophilic, ambiphilic reaction center.

lent case, a predominantly electrophilic molecule forms a π-bound adduct *via* Lewis basic lone pair donation by a P_4 phosphorus atom to an empty *p*-orbital at the reaction center. This zwitterionic adduct can then undergo electronic rearrangement to a tetraphosphabicyclobutane-based structure (Scheme 5.1.2). Examples of ambiphilic systems that are predominantly electrophilic include silylenes and aluminum (I) species. The low valent atoms in these heavier element systems typically have a lower energy lone pair (i.e. not the HOMO) and thus tend to initially react *via* the low-lying empty orbital. A recent systematic study on the electronic structures of main-group carbene analogues clearly outlines this energetic trend [113]. Calculations performed on the mechanism of the nucleophilic stage indicate the inclusion of a second stabilizing P_4 in the transition state, lowering the activation energy of the rearrangement process [112,114–117]. To our knowledge, no experimental evidence of a bimolecular mechanism involving two P_4 molecules has been reported in the literature.

Activation of P_4 may also be facilitated by those ambiphilic molecules dominated by nucleophilic character. This class of molecules is exemplified by singlet carbenes. These systems are known for being strong σ-donors through the lone pair of electrons as well as having electrophilic character at the carbene center. Those reactions initiated by nucleophilic attack of a vacant P_4 *p*-orbital are followed by an electrophilic stage in which electronic rearrangement of the intermediate yields a cyclotriphosphene unit (Scheme 5.1.3) [112,114]. To date, this type of reactivity has been limited to singlet carbenes in the literature [118–120].

5.2. Electrophile initiated, ambiphilic activation of P_4

5.2.1. Group 13

The Group 13 molecules that activate P_4 through an ambiphilic mechanism are dominated by electrophilic character at the active site [113]. As stated in the preceding section, an electrophilic initiated reaction pathway including electron donation from the P_4 molecule to an empty *p*-orbital of the activating species forming a π-complex should occur. In this section examples of Group 13 reactivity will encompass basic electrophilic dominated ambiphilic reaction mechanisms by which complex fragmentation and/or derivatization of P_4 may subsequently take place.

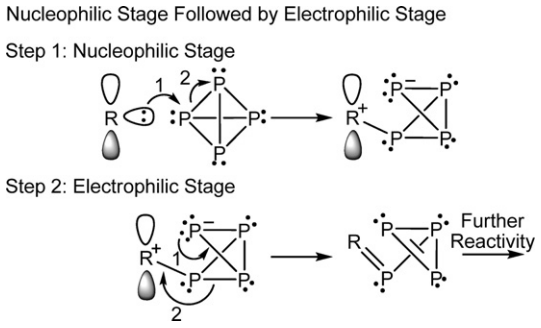

Scheme 5.1.3. Proposed mechanism for the activation of P_4 by a predominantly nucleophilic, ambiphilic molecule.

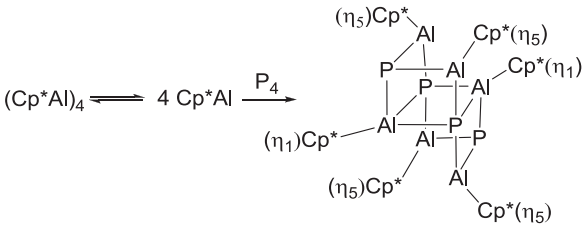

Scheme 5.2.1.1. Dissociation of the tetrameric $(Cp^*Al)_4$ in solution and subsequent P_4 activation.

Tetrameric pentamethylcyclopentadienyl aluminum(I) $(Cp^*Al)_4$, is in equilibrium with monomeric Cp*Al in toluene [121,122]. Reaction of $(Cp^*Al)_4$ with P_4 generates a product of the formula $(Cp^*Al)_6P_4$ (Scheme 5.2.1.1). The single crystal structure revealed the Cp* fragments of the Al_6P_4 based product are present in both η^5- and η^1-binding modes (Fig. 5.2.1.1). As to elucidate the nature of the unusual bonding arrangement observed in this molecule, SCF calculations were performed on C_{2h}, C_{3v}, and T_d symmetry based $P_4(Cp^*Al)_6$ frameworks. The results indicate each phosphorus atom carries a weakly delocalized 3s lone pair of electrons which contribute to the stabilization of nonbonding Al–Al interactions, thermodynamically favoring the rearrangement of other symmetry based cages into the structurally characterized product [123].

In a second instance of low valent aluminum activation, Roesky et al. employed a β-diketiminate derivative, the monomeric NacnacAl(I), to facilitate insertion into the P_4 tetrahedron (Scheme 5.2.1.2). Reactivity at the aluminum(I) center forms a bridged dimeric species through two cycles of electrophilic insertion. The structure of the product was confirmed through single crystal X-ray analysis (Fig. 5.2.1.2). DFT calculations performed on the electronic structure of the product indicate significant charge transfer (-0.22 e$^-$) from the aluminum centers and the presence of predominantly ionic Al–P bonds [124].

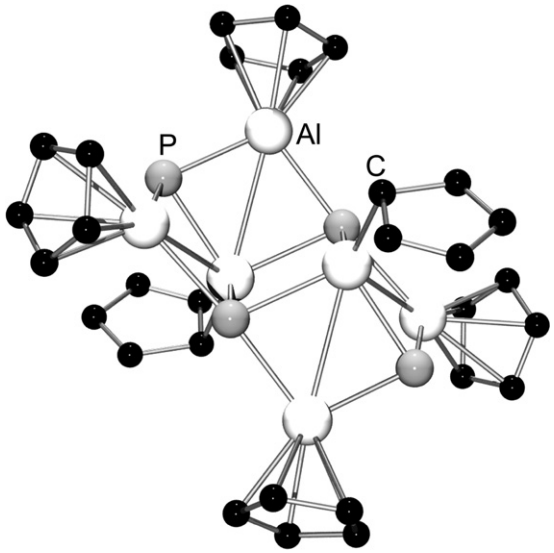

Fig. 5.2.1.1. Solid state structure of $P_4(Cp^*Al)_6$ [123]. Hydrogen atoms and Cp* methyl-groups are omitted for clarity.

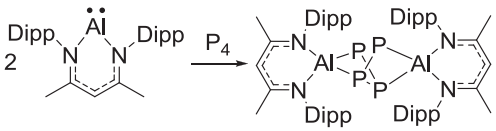

Scheme 5.2.1.2. Activation of white phosphorus *via* NacnacAl(I) forming a bridging dimeric species.

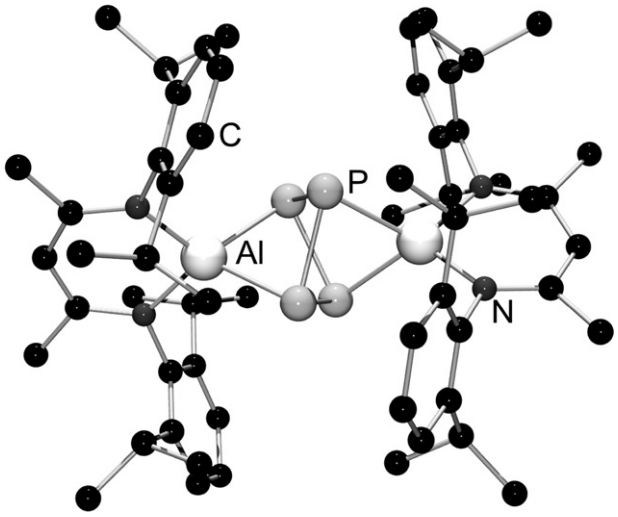

Fig. 5.2.1.2. Solid state structure of $(NacnacAl)_2P_4$ [124]. Hydrogen atoms are omitted for clarity.

In the most recent published work concerning gallium activation of P_4, Prabusankar et al. have utilized NacnacGa(I) ($CH(C(Me)(N\text{-}^iPr_2C_6H_3))_2Ga$) in a similar fashion to the aluminum species depicted in Scheme 5.2.1.2; isolating the tetraphosphabicyclobutane intermediate and functionalizing the product with molybdenum pentacarbonyl [125]. Interestingly, the bridged dimeric species seen in the case of NacnacAl(I) is not observed, permitting the formation of a bis-molybdenum pentacarbonyl adduct. The authors do not speculate on the inconsistent reactivity among the NacnacAl(I) and NacnacGa(I) (Fig. 5.2.1.3 and Scheme 5.2.1.3).

Activation of white phosphorus *via* low valent alkylgallium(I) species is also evident in the literature. As in the case of tetrameric $(AlCp^*)_4$ [123], tetrameric $(GaC(SiMe_3)_3)_4$ can dissociate into

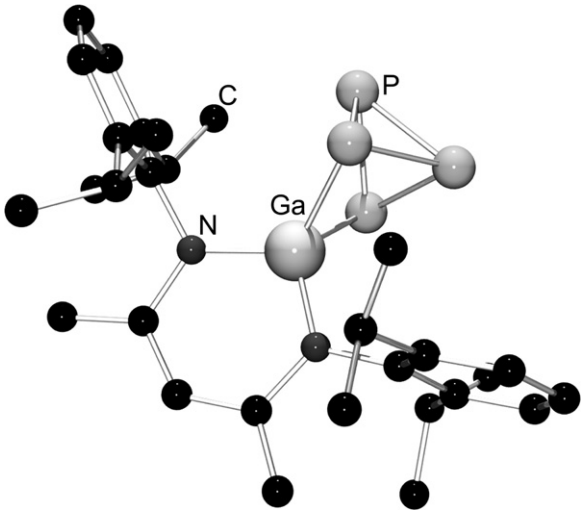

Fig. 5.2.1.3. Solid state structure of $NacnacGaP_4$ [125]. Hydrogen atoms are omitted for clarity.

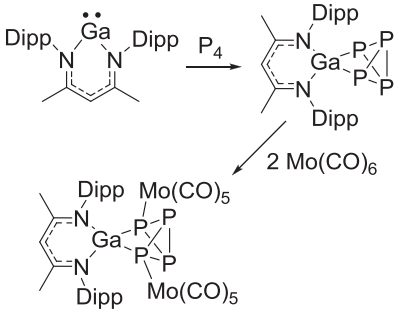

Scheme 5.2.1.3. Activation of white phosphorus *via* NacnacGa(I) and derivatization using molybdenum hexacarbonyl.

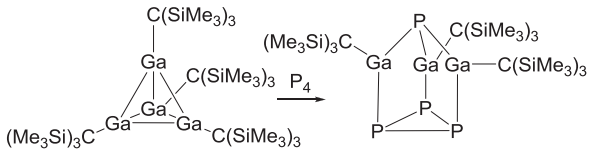

Scheme 5.2.1.4. Formation the $P_4Ga_3[C(SiMe_3)]_3$ complex through triple insertion of P_4 with monomeric $GaC(SiMe_3)_3$.

monomeric $GaC(SiMe)_3$ in solution and undergo a triple insertion reaction with white phosphorus (Scheme 5.2.1.4) [126,127]. The solid state structure (Fig. 5.2.1.4) of the product contains a three phosphorus atom homocycle in which each phosphorus atom is attached to a single gallium in the second planar region of the structure. The fourth phosphorus resides above the secondary gallium layer in a triangular prism-like arrangement. Of note is the apical phosphorus atom, which has a chemical environment rarely observed in the literature appearing as a quartet with a chemical shift of −521.9 ppm in the ^{31}P NMR spectrum, a region usually reserved for white phosphorus itself.

5.2.2. Group 14

In a preliminary case of silicon-based P_4 chemistry, activation is achieved *via* sterically hindered disilenes. Partial fragmentation of P_4 with silenes results in a 1,3-diphospha-2,4-disilabicyclo-[1.1.0]butane core. To this effect, 2,2,4,4-tri-mesityl-1,3-diphospha-2,4-disilabicyclo-[1.1.0]butane and other fragmen-

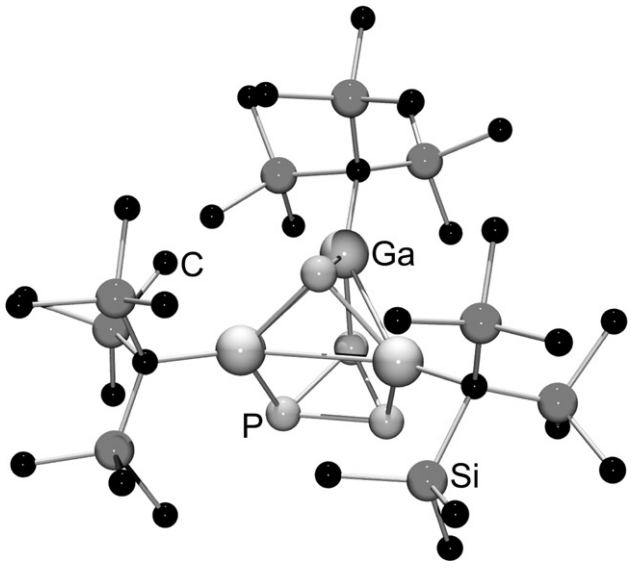

Fig. 5.2.1.4. Solid state structure of $P_4Ga_3[C(SiMe_3)]_3$ [127]. Hydrogen atoms are omitted for clarity.

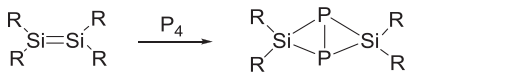

R = Mes, 2,6-dimethylphenyl, 2,6-di-methyl-4-*tert*-butylphenyl

Scheme 5.2.2.1. Fragmentation of P_4 *via* sterically bulky tetrasubstituted-disilenes.

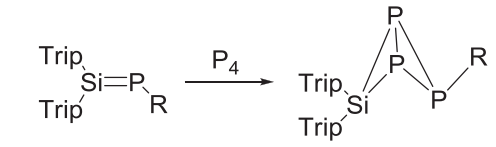

R = $SiMe_3$, ^{t}Bu, Si^iPr_3

Scheme 5.2.2.2. Activation of P_4 using bulky phosphasilenes.

tation products are formed by the addition of P_4 to tetramesityl- and other bulky disilylenes [128,129] (Scheme 5.2.2.1). To respond to the extent that sterics play a role in the silene mediated activation, an even bulkier organosilene, tetrakis(2,4,6-tri-*iso*-propylphenyl)phosphadisilene, did not successfully functionalize P_4 [129].

The increased steric bulk affecting the reactivity of the symmetrical disilenes may be mediated by substitution of one organosilene moiety with an organophosphene. In this case, crowded phosphasilenes are successful in fragmenting P_4, yielding products similar to the less bulky disilenes in the 1,3,4-tri-phospha-2-silabicyclo-[1.1.0]butane mold [130] (Scheme 5.2.2.2).

This reactivity pattern can be applied to non-symmetrical disilenes as well with the potential to produce both the *exo–endo* and *exo–exo* conformers. In this case, *E*-1,2-dimesityl-1,2-di-*tert*-butyldisilene reacts with P_4 forming two symmetrically inequivalent products. Interestingly, the type of reactivity displayed between disilenes and P_4 is uncommon in normal disilene chemistry as both the silicon–silicon σ- and π-bonds are broken and new silicon–phosphorus single bonds are formed in the product [129] (Scheme 5.2.2.3).

In reactivity similar to that of the monomeric Nacnac aluminum(I) species in Scheme 5.2.1.2, the monomeric silylene, LSi(II) (L = CH[(C = CH_2)CMe][N(2,6-^{i}Pr$_2$C$_6$H$_3$)]$_2$), reacts with white phosphorus in a step-wise manner (Scheme 5.2.2.4). Unlike NacnacAl(I), the 1:1 intermediate can be isolated (Fig. 5.2.2.1). Furthermore, addition of a second equivalent of silylene results in the insertion of a second Si center into a P–P bond (Fig. 5.2.2.2) [131,132] (Scheme 5.2.2.4).

5.2.3. Group 15

Phosphenium ions are the two coordinate, cationic cousins of carbenes which display ambiphilic character as they are both Lewis acids and Lewis bases. The stability of these cations depends on the π-donation by the ligand groups into the empty *p*-orbital of the phosphorus center and the polarization of the σ-bond.

Beginning with Krossing et al. in 2001 the functionalization of P_4 was completed using the insertion of an *in situ* generated predominantly electrophilic [PR_2]$^+$ cation (R = Br, I) into the P_4 tetrahedron [133,134]. Polyphosphorus cations were isolated and structurally characterized with the formation of a binary, cationic phosphorus

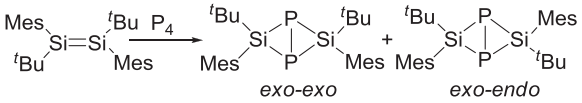

Scheme 5.2.2.3. Fragmentation of P_4 using a non-symmetrical disilene.

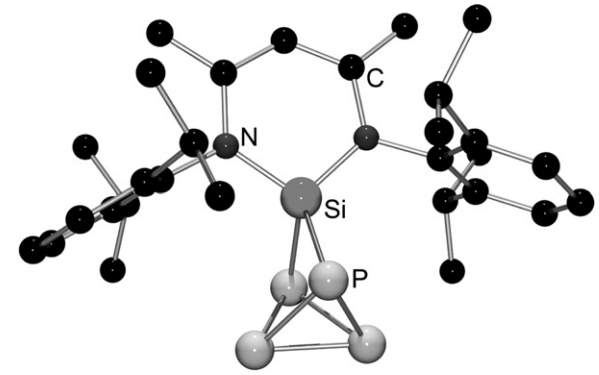

Fig. 5.2.2.1. Solid state structure of L-SiP_4 (L = CH[(C = CH_2)CMe][N(2,6-^{i}Pr$_2$C$_6$H$_3$)]$_2$) [132]. Hydrogen atoms are omitted for clarity.

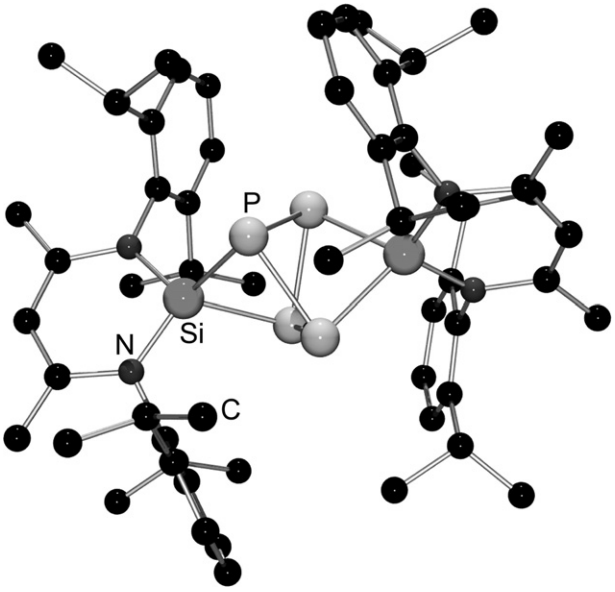

Fig. 5.2.2.2. Solid state structure of (L-Si)$_2$$P_4$ (L = CH[(C = CH_2)CMe][N(2,6-^{i}Pr$_2$C$_6$H$_3$)]$_2$) [132]. Hydrogen atoms are omitted for clarity.

cage [P_5X_2]$^+$ along with a weakly coordinating aluminum anion Al[OC(CF_3)$_3$]$_4^-$ (Fig. 5.2.3.1 and Scheme 5.2.3.1).

On a similar line of investigation by Krossing et al., the formation of the P_5^+ monocation as an intermediate to the aforementioned $P_5I_2^+$ cation as well as the newly proposed $P_3I_6^+$ cation was established. The P_5^+ intermediate was characterized through ^{31}P NMR data as well as *ab initio* calculations. Although these reactions may be completed using P_4 as a reagent, a more efficient secondary route through a silver aluminate salt to the reported cationic phosphorus species is also possible [134] (Scheme 5.2.3.2).

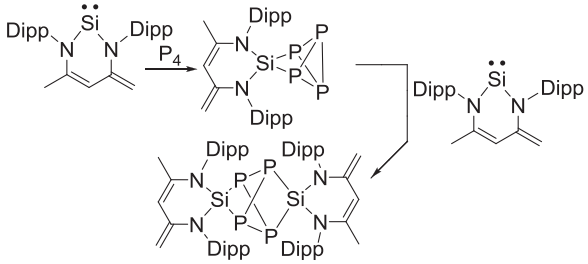

Scheme 5.2.2.4. Activation of P_4 by a low valent, monomeric silylene.

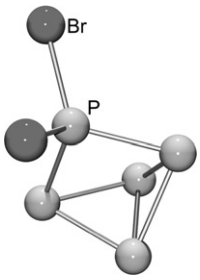

Fig. 5.2.3.1. Solid state structure of $[P_5Br_2]^+$ cation [133]. The $[Al(OC(CF_3)_3)_4]^-$ anion has been omitted for clarity.

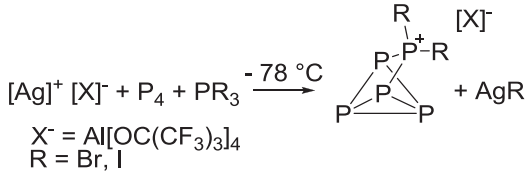

Scheme 5.2.3.1. Formation of binary cationic phosphorus cages through P_4 activation.

More recently, in work by Weigand et al., phosphenium ions were prepared *in situ* by gallium (III) chloride induced halide abstraction from chlorodiphenylphosphine, and subsequently used to activate P_4. Under varying reaction conditions, stoichiometric ratios of the starting materials and excess P_4, preparation of three new cationic phosphorus species was reported [135]. A molten reaction media with varying proportions of P_4:Ph_2PCl:$GaCl_3$ were utilized in a solvent-free method resulting in the isolation of mono-($[Ph_2P_5]^+$), di-($[Ph_4P_6]^{2+}$) and tri-($[Ph_6P_7]^{3+}$) cationic phosphorus species. The solid state structures of $[Ph_2P_5][GaCl_4]$ (Fig. 5.2.3.2) and $[Ph_6P_7][GaCl_4]_3$ (Fig. 5.2.3.3) were determined. The solvent-free, molten reaction medium was required due to the propensity of phosphenium ions to interact with solvent molecules as is seen in the case of CH_2Cl_2 interfering with reactivity [134]. In the case of the $[P_7Ph_6]^{3+}$ cation, an increased ratio of $GaCl_3$ was required to produce an overall acidic media for the reaction to occur without the presence of potentially detrimental and nucleophilic $[Cl]^-$ ions in the melt (Scheme 5.2.3.3).

Phosphenium ion mediated activation of white phosphorus is also effective using the cation derived from the *cyclo*-1,3-diphospha-2,4-diazane $(DippNPCl)_2$. The resulting intermediate allowed for the targeted preparation of new mono- and dicationic phosphorus species. *In situ* preparation of the phosphenium ions in fluorobenzene utilizing gallium(III) chloride as a halide abstractor allowed the mono- and dicationic molecules to activate one or two equivalents of white phosphorus, respectively (Scheme 5.2.3.4) [136]. The crystal structures of both products are shown in Figs. 5.2.3.4 and 5.2.3.5.

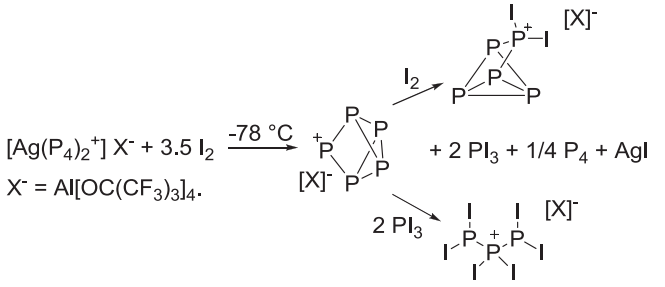

Scheme 5.2.3.2. Formation of the P_5^+ intermediate in the synthesis of $P_5I_2^+$ and $P_3I_6^+$ phosphenium ions.

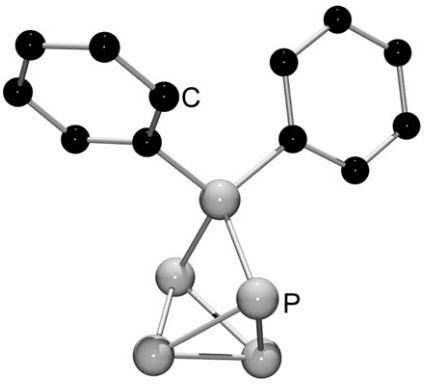

Fig. 5.2.3.2. Solid state structure of $[Ph_2P_5][GaCl_4]$ [135]. Hydrogen atoms and weakly coordinating tetrachlorogallate anion are removed for clarity.

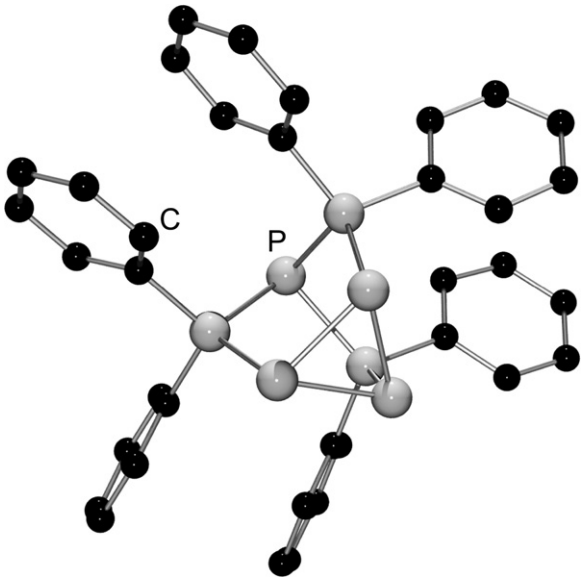

Fig. 5.2.3.3. Solid state structure of $[Ph_6P_7][GaCl_4]_3$ [135]. Hydrogen atoms and weakly coordinating tetrachlorogallate anions are removed for clarity.

5.3. Nucleophile initiated, ambiphilic activation of P_4

Nucleophilic, yet electrophilic carbenes activate the P_4 tetrahedron through nucleophilic attack of an empty *p*-orbital of a P_4 phosphorus atom, complying with the reactivity pattern outlined in Scheme 5.1.3. Ring opening nucleophilic attack will then be

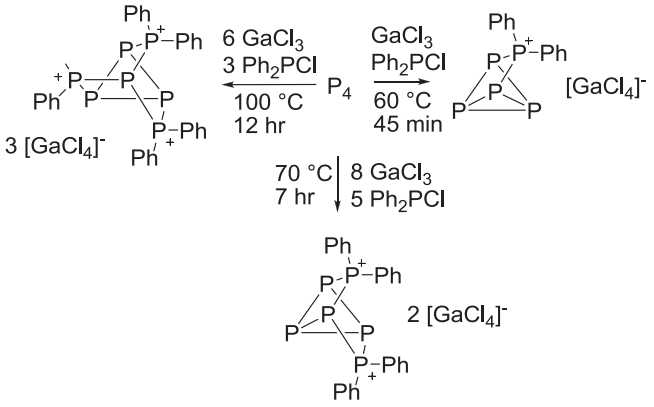

Scheme 5.2.3.3. Formation of $[P_5Ph_2][GaCl_4]$, $[P_6Ph_4][GaCl_4]_2$ and $[P_7Ph_6][GaCl_4]_3$ *via in situ* generated phosphenium ions.

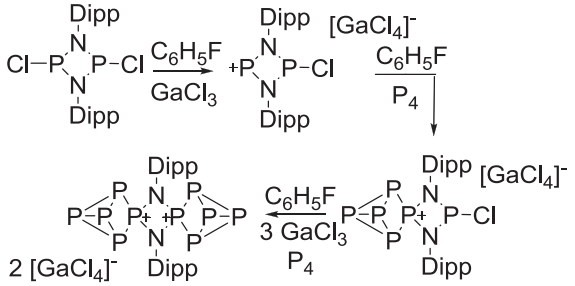

Scheme 5.2.3.4. Preparation of mono- and dicationic phosphorus *cyclo*-1,3-diphospha-2,4-diazane molecules.

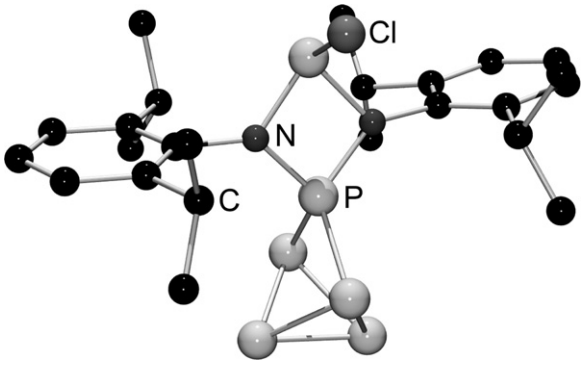

Fig. 5.2.3.4. Solid state structure of $[P_4(DippNP)_2Cl][GaCl_4]$ [136]. Hydrogen atoms and weakly coordinating tetrachlorogallate anion are removed for clarity.

followed by a stabilizing electrophilic rearrangement to a cyclotriphosphirene intermediate.

The principal difference between the corresponding silylene and carbenes is that silicon is a heavier element homologue of carbon in which the valence *s*-orbital is exceedingly contracted and lower in energy compared to its valence *p*-orbital and is therefore reluctant to hybridize, dictating electrophilic behavior of silylenes compared to carbenes [112]. Secondly, donation of electrons from the amino substituents to the vacant *p*-orbital is much more efficient in the case of carbenes as the vacant *p*-orbital on carbon achieves greater efficiency in orbital overlap with the donating nitrogen lone pairs. This lack of overall electron density at the silylene center manifests itself as high activation energy barriers and lower efficiency in nucleophilic insertion reactions [117].

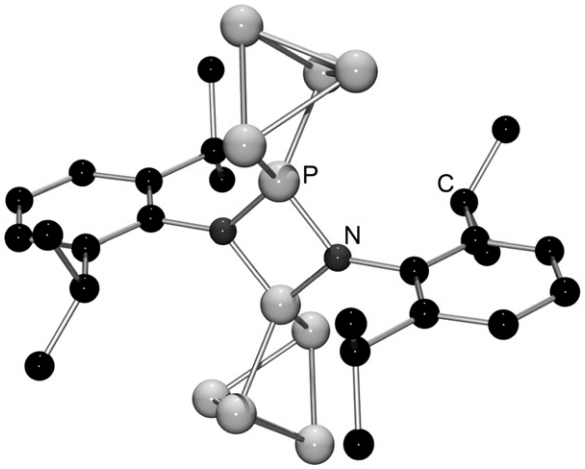

Fig. 5.2.3.5. Solid state structure of $[P_4(DippNP)_2P_4][GaCl_4]_2$ [136]. Hydrogen atoms and weakly coordinating tetrachlorogallate anions are removed for clarity.

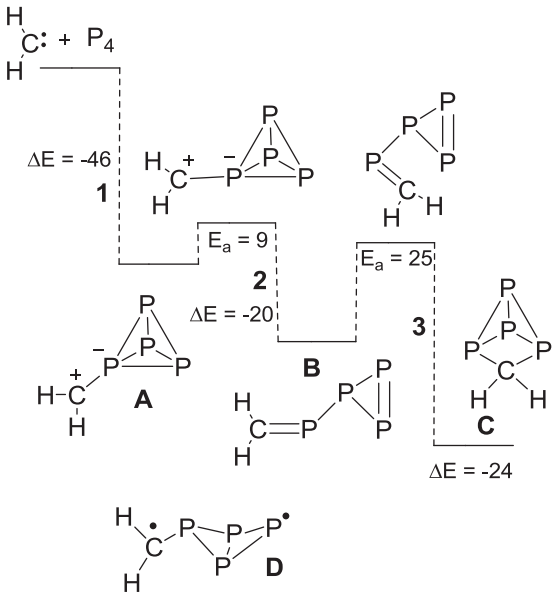

Scheme 5.3.1. Profile for the reaction of P_4 with methylene. Energies are in kcal/mol.

Calculations at the B3LYP/6-311++G(3df,3p)//B3LYP/6-311++G(3df,3p) level on the reactivity of singlet and triplet methylene with P_4 do not attribute these small, π-donor free carbenes as being electrophilic [116]. The reactivity of singlet methylene is based on the empty *p*-orbital unlike the case of common NHCs which are strong σ-donors [137]. As a consequence, singlet methylene forms a bicyclic structure with P_4 as is expected with electrophilic molecules with the highest energy structure being the initial π-complex formed when acting as an electrophile. The reaction pathway is as follows (Scheme 5.3.1): 1. There is no transition state between $CH_2 + P_4$ and the structure **A** ($\Delta E = -46$ kcal/mol); 2. Next the cyclotriphosphirene **B** forms ($E_a = 9$ kcal/mol, $\Delta E = -20$ kcal/mol); 3. The insertion product **C** is formed *via* a transition state where the $H_2C{=}P$ fragment twists about the P–P bond ($E_a = 25$ kcal/mol, $\Delta E = -24$ kcal/mol). At the same level of calculation, methylene has a low singlet–triplet gap of −9 kcal/mol, suggesting the triplet state may play an important role in reactivity. However, careful analysis resulted in only one stable, high-energy structure **D** (19 kcal/mol higher in energy than **C**). This structure is highly reminiscent of the expected radical-reactivity with white phosphorus with formation of a tetraphosphabicyclo[1.1.0]butane. There are two unpaired electrons in this structure: one located on the carbon atom and one located on the two-coordinate phosphorus atom [116].

Stable cyclic alkyl-amino carbenes (CAACs) have been shown in the literature to exhibit behavior similar in reactivity to that of transition metals [138]. When allowed to react with P_4, the large (menthyl)CAAC produces a P_4 core fragment which is essentially planar and is coplanar with the CAAC rings yielding the first example of a stable 2,3,4,5-tetraphosphatriene (Scheme 5.3.2 and Fig. 5.3.1) [118].

The diphosphene core of 2,3,4,5-tetraphosphatriene undergoes a [4+2] cycloaddition reaction with 2,3-dimethylbutadiene (Scheme 5.3.2 and Fig. 5.3.2). The formation of the new P–C bonds occurs with high diastereoselectivity. Calculations at the B3LYP/6-311g(d,p) level show that the reaction of CAAC with P_4 follows a similar mechanism, as proposed in Scheme 5.3.1. Nucleophilic attack of the parent CAAC molecule with P_4 results in the formation of a triphosphirene intermediate ($E_a = 3.6$ kcal/mol, $\Delta E = -18.3$ kcal mol). A second CAAC molecule attacks one of the two coordinate triphosphirene molecules with no reac-

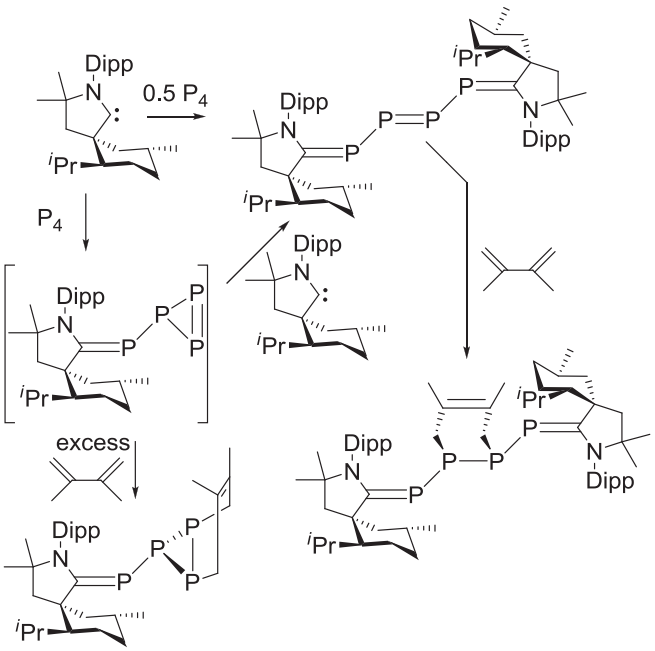

Scheme 5.3.2. Nucleophilic insertion of a cyclic alkyl-amino carbene into P_4 and subsequent hetero Diels-Alder [4 + 2] cycloaddition reactions.

tion barrier, forming a zwitterionic intermediate which then rearranges with minimal barrier (E_a = 3.8 kcal/mol) to the 2,3,4,5-tetraphosphatriene (ΔE = −11 kcal/mol). Attempts to trap the triphosphirene intermediate were successful. Addition of (menthyl)CAAC to a mixture of white phosphorus and a gross excess of 2,3-dimethylbutadiene resulted in the quantitative formation of the [4 + 2] cycloaddition product as a single diastereoisomer (Scheme 5.3.2 and Fig. 5.3.3).

In the case of an *N*-heterocyclic carbene (NHC), reactions with white phosphorus initially follow that of the (menthyl)CAAC. Trapping reactions with 2,3-dimethylbutadiene confirmed the presence of the triphosphirene intermediate as well as the formation of the 2,3,4,5-tetraphosphatriene (Scheme 5.3.3). The solid state structures of these products are shown in Figs. 5.3.4 and 5.3.5. However,

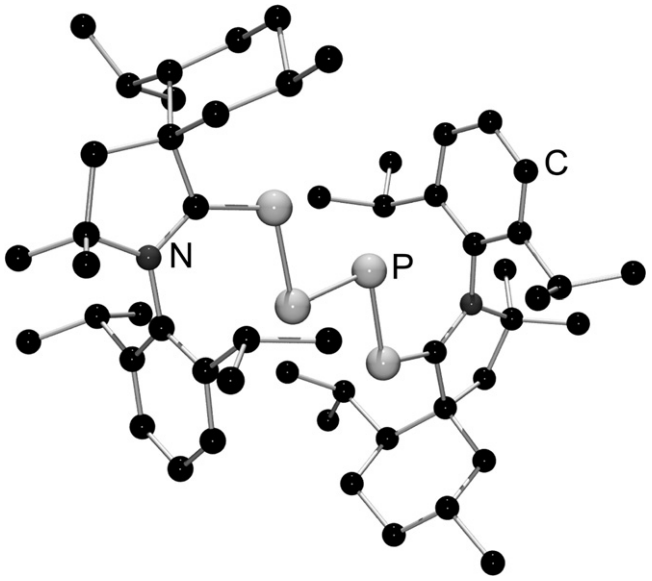

Fig. 5.3.1. Solid state structure of the (menthyl)CAAC-capped 2,3,4,5-tetraphosphatriene [118]. Hydrogen atoms are omitted for clarity.

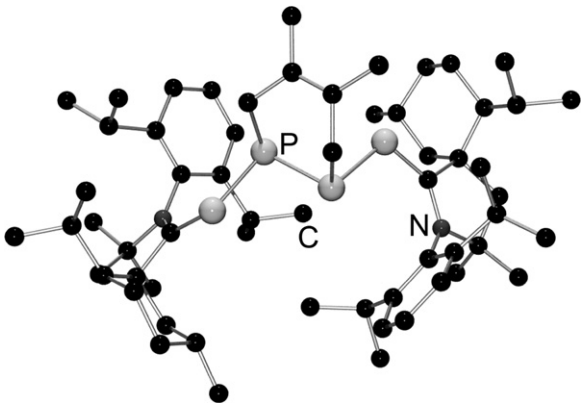

Fig. 5.3.2. Solid state structure of the cycloaddition product of (menthyl)CAAC-capped 2,3,4,5-tetraphosphatriene and 2,3-dimethylbutadiene [118]. Hydrogen atoms are omitted for clarity.

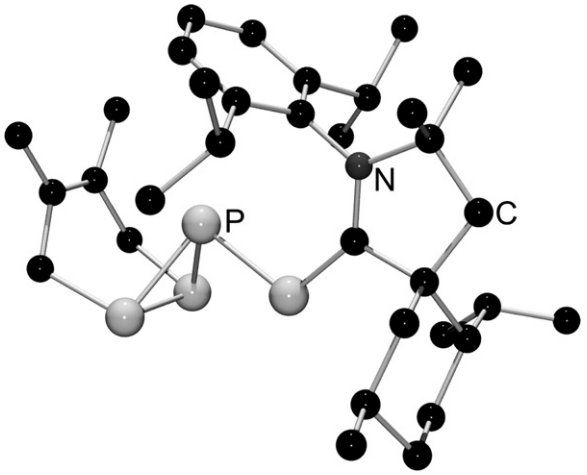

Fig. 5.3.3. Solid state structure of the [4 + 2] cycloadditon product of triphosphirene and 2,3-dimethylbutadiene [118]. Hydrogen atoms are omitted for clarity.

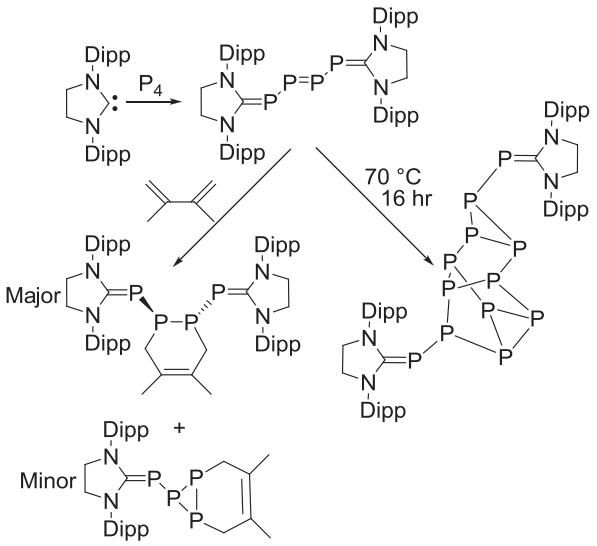

Scheme 5.3.3. Reactivity of a singlet NHC with P_4 and subsequent [4 + 2] cycloaddition.

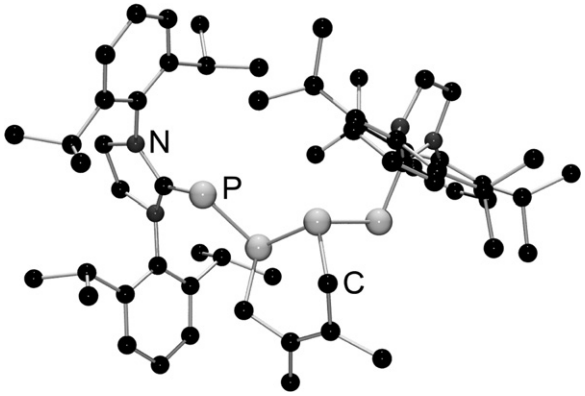

Fig. 5.3.4. Solid state structure of the cycloaddition product of NHC-capped 2,3,4,5-tetraphosphatriene and 2,3-dimethylbutadiene [119]. Hydrogen atoms are omitted for clarity.

attempts to isolate the 2,3,4,5-tetraphosphatriene were unsuccessful due to the slow formation of another product at room temperature. In this case, extended reaction times or elevated temperatures allow for the aggregation of P_4 to form a P_{12} cluster capped by two NHC fragments (Scheme 5.3.3). The difference in reactivity between the NHC and CAACs is attributed to the greater electrophilic character of the central carbon atom in the latter, stabilizing the resulting phosphaalkene. *N*-heterocyclic carbenes are generally less Lewis acidic and make better leaving groups, permitting aggregation of the P_{12} core [119]. The polycyclic structure observed is similar to those organosubstituted polyphosphines and polyphosphorus anions described by Baudler and Glinka [13]. The P_{12} core contains three five-membered rings, two three-membered rings, one six-membered ring and is unprecedented in the literature as a dodecaphosphine (Fig. 5.3.6) [119].

The mechanism of the P_{12} cluster formation was studied through calculations at the B3LYP/6-311G** level (Scheme 5.3.4). The study indicated that the 2,3,4,5-tetraphosphatriene and triphosphirene intermediates undergo a formal [3+2] cycloaddition reaction (E_a = 0 kcal/mol, ΔE = −13.3 kcal/mol). Elimination of two NHC fragments and rearrangement to a heptaphosphanorbornadiene intermediate provides a pathway through which an additional triphosphirene can add without reaction barrier through a [$\pi^2 + \pi^2 + \pi^2$] reaction, yielding the structurally characterized P_{12} containing product (ΔE = −54.9 kcal/mol) [119].

To further study the reactivity of singlet carbenes with P_4 beyond activation and aggregation, Betrand et al. proposed the use of smaller, alkyl amino carbenes to induce further fragmentation. In this case an acyclic alkyl amino carbene and cyclohexyl CAAC were chosen [138–140]. The results indicate that the acyclic alkyl amino carbene is sufficiently nucleophilic to ring open the P_4 cage, forming the triphosphirene intermediate. This intermediate then undergoes insertion of a second carbene into the P=P double bond (Scheme 5.3.5). The connectivity was confirmed by the single crystal X-ray structure (Fig. 5.3.7) [120].

The (cHex)CAAC was successful in inducing activation and partial fragmentation of P_4 yielding P_4[(cHex)CAAC]$_3$ (major product) and P_2[(cHex)CAAC]$_2$ (minor product) from the reaction with P_4 (Scheme 5.3.6) [120]. The single crystal X-ray structures confirmed the formation of the proposed products (Figs. 5.3.8 and 5.3.9).

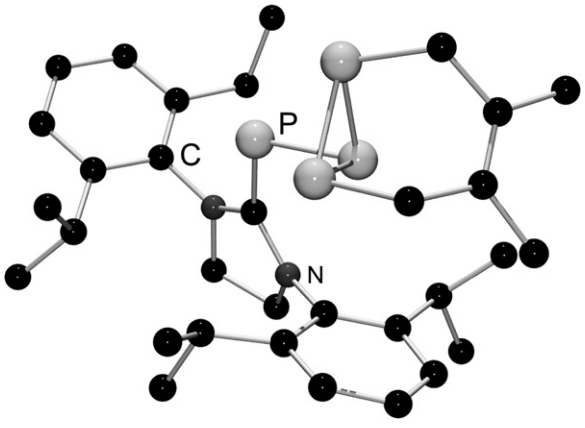

Fig. 5.3.5. Solid state structure of the [4+2] cycloadditon product of NHC-triphosphirene and 2,3-dimethylbutadiene [119]. Hydrogen atoms are omitted for clarity.

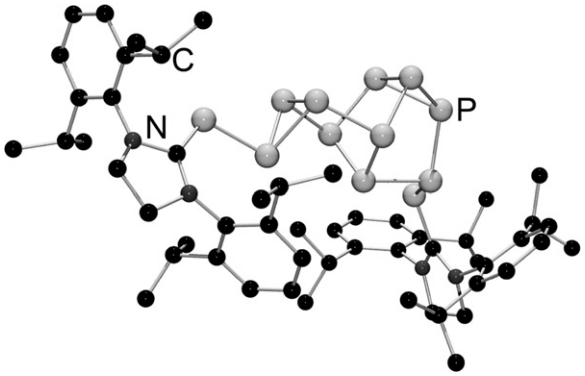

Fig. 5.3.6. Solid state structure of a dodecaphosphine-bridged *N*-heterocyclic carbene and P_4 product [119]. Hydrogen atoms are omitted for clarity.

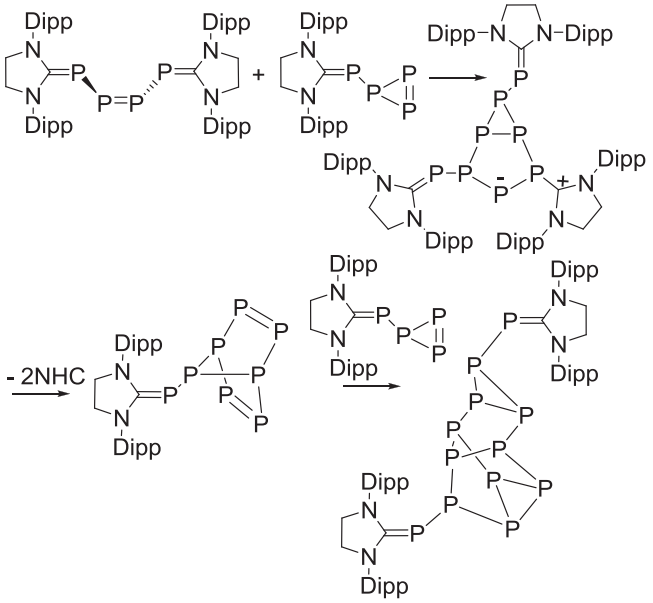

Scheme 5.3.4. Proposed mechanism for the formation of the P_{12} core in Bertrand's bis-NHC dodecaphosphine.

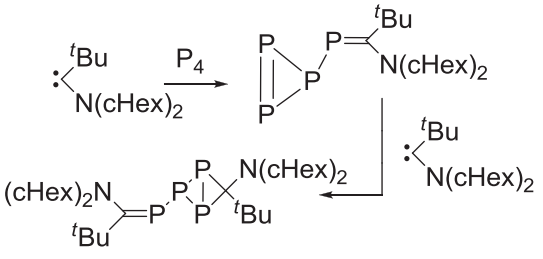

Scheme 5.3.5. Reaction of bis(cyclohexyl)amino-*tert*-butyl carbene with P_4.

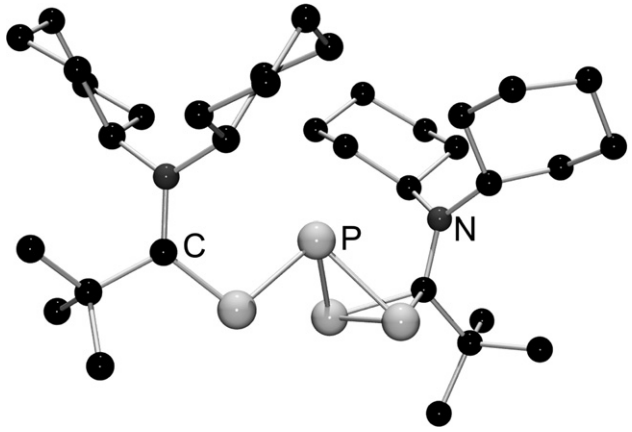

Fig. 5.3.7. Solid state structure of the double insertion product of bis(cyclohexyl)amino-*tert*-butyl carbene into P_4 [120]. Hydrogen atoms are omitted for clarity.

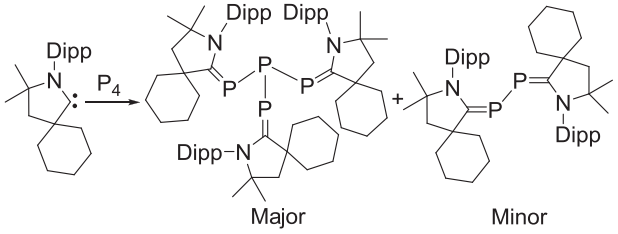

Scheme 5.3.6. Reaction of cyclohexyl CAAC with white phosphorus facilitating partial fragmentation of P_4.

The differing reactivity can be rationalized as the (cHex)CAAC is considerably sterically smaller than the (menthyl)CAAC. Although it is difficult to compare the size of the (cHex)CAAC with bis(cyclohexyl)amino-*tert*-butyl carbene from the previous example, the reactivity differences can be accounted for electronically as the acyclic carbene is one of the most electrophilic isolable carbenes [120,139]. With this in mind, it is reasonable to conclude that after the addition of two acyclic carbenes the reaction stops due to the stability of the three membered P–P–C ring. Since the (cHex)CAAC is less electrophilic, additional carbene substitution and fragmentation of the P_4 core is possible [120].

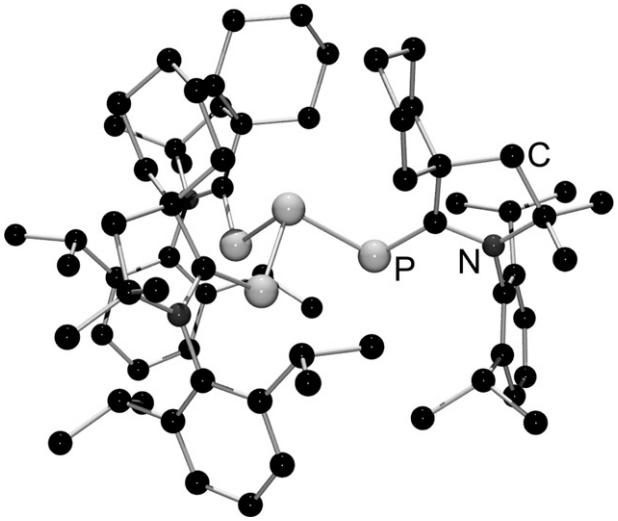

Fig. 5.3.8. Solid state structure of $(CAAC)_3P_4$ [120]. Hydrogen atoms are omitted for clarity.

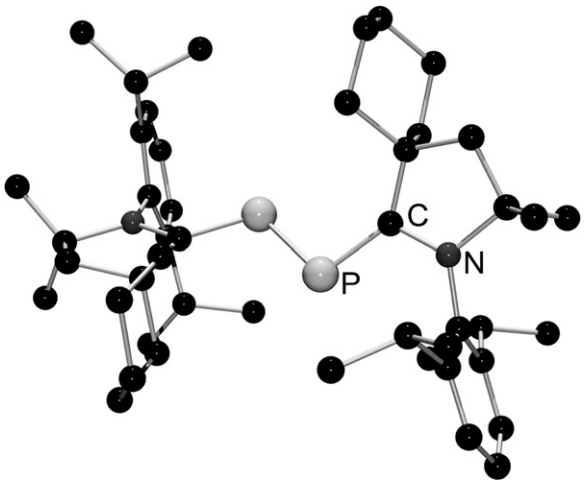

Fig. 5.3.9. Solid state structure of $(CAAC)_2P_2$ [120]. Hydrogen atoms are omitted for clarity.

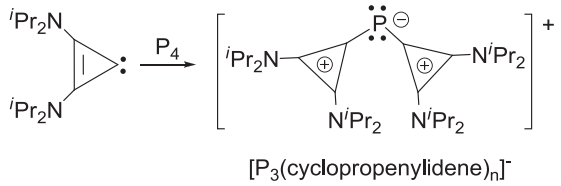

Scheme 5.3.7. Reaction of bis(di-*iso*-propylamino)cyclopropenylidene with P_4 resulting in P_4 fragmentation.

Further fragmentation was then achieved by utilizing the least sterically demanding, nucleophilic carbene in the literature [141]. Bis(di-*iso*-propylamino)cyclopropenylidene reacts with P_4 to form a cationic species containing one phosphorus atom bound to two cyclopropenylidenes with an ill-defined $[P_3(cyclopropenylidene)_n]^-$ anion (Scheme 5.3.7) [120]. Although this species was not structurally characterized by single crystal X-ray diffraction techniques, in the presence of chloroform a product could be isolated that had the same ^{31}P NMR signal as the [P(cyclopropenylidene)$_2$] cation and a chloride anion. The solid state structure from this material is shown in Fig. 5.3.10.

6. Reactions with *p*-block radicals

Investigations into the reactivity of white phosphorus with *p*-block radicals appears to be in its infancy and as will be shown in the following section, there is potential for discoveries in this area. Reactions of white phosphorus with radicals typically follow

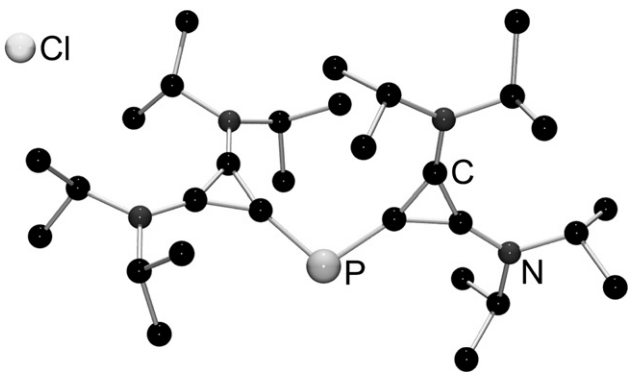

Fig. 5.3.10. Solid state structure of the Bis(di-*iso*-propylamino)cyclopropenylidene and P_4 product [120]. Hydrogen atoms are omitted for clarity.

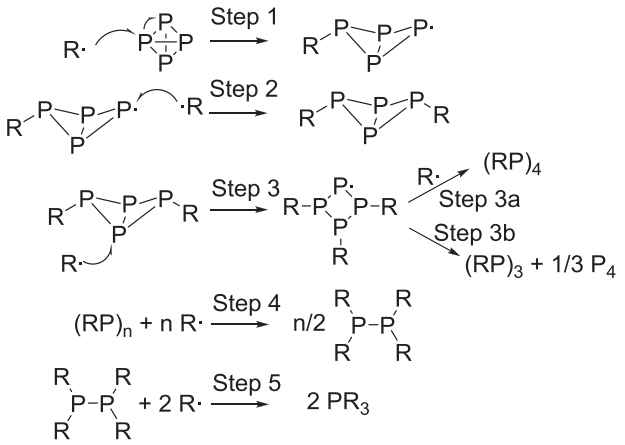

Scheme 6.1. Possible reaction mechanisms for reaction of white phosphorus with radical species.

the following steps (Scheme 6.1): Step 1, radical attack at a phosphorus atom with concomitant breakage of one P–P bond resulting in the opening of the white phosphorus tetrahedron and formation of a phosphorus-based radical; Step 2, a second radical reacts forming a tetraphosphabicyclo[1.1.0]butane-based species; Step 3, a third radical would then presumably attack one of the bridging phosphorus atoms in the tetraphosphabicyclo[1.1.0]butane core with breakage of the P–P bridge and formation of a four-membered phosphorus ring. This species can then: (a) react with another radical to form an $(RP)_4$ species or (b) eject a phosphorus atom and ring close to form $(RP)_3 + 1/3\ P_4$; Step 4, Further reaction with radicals would result in degradation of the $(RP)_n$ rings and form $R_2P–PR_2$; and Step 5, final reaction of radical species with $R_2P–PR_2$ results in the formation of the tertiary phosphine. Clearly the formation of these species will be highly dependent on the electronic, and in particular, the steric requirements of the radical-containing species. However, in some cases, a concerted reaction mechanism cannot be excluded where a P–P bond of white phosphorus adds across an element–element bond *via* a four-centered transition state. As seen in the following examples the tetraphosphabicyclo[1.1.0]butane-based species from Step 2 is often the main isolated product due to the large substituents on the radical species.

Insights into the oxidation reaction of white phosphorus with halogens were determined by ^{31}P NMR spectroscopy [142]. It is interesting to note that the reaction of P_4 with bromine in a 2:1 molar ratio results in the formation of small amounts of the butterfly-like compounds *exo*,*exo*-dibromotetraphosphabicyclo[1.1.0]butane and *exo*,*endo*-dibromotetraphosphabicyclo[1.1.0]butane. It was speculated that these were intermediates in the production of P_2Br_4 and PBr_3. The formation of these species is likely through a radical-type of route as outlined in steps 1 and 2 above (Scheme 6.1), where homolytic cleavage of the Br–Br bond yields two bromine radicals which then attack the P_4 tetrahedron in a step-wise manner. These tetraphosphabicyclo[1.1.0]butanes were not isolated due to their thermal instability with a half-life of approximately 1 h (Scheme 6.2).

In 2004, Lappert et al. reported that upon heating, the diphosphine $[(^iPr_2N)(Me_3Si)_2NP]_2$ underwent reversible dissociation into the phosphinyl radical $(^iPr_2N)(Me_3Si)_2NP^•$ [143]. The reaction of the diphosphine with white phosphorus over 1.5 h in refluxing

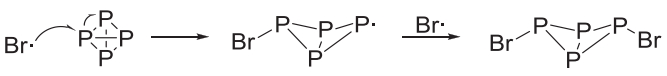

Scheme 6.2. Radical reaction of bromine with white phosphorus.

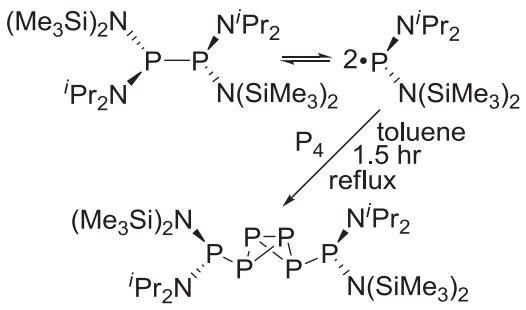

Scheme 6.3. Reaction of a phosphinyl radical with white phosphorus.

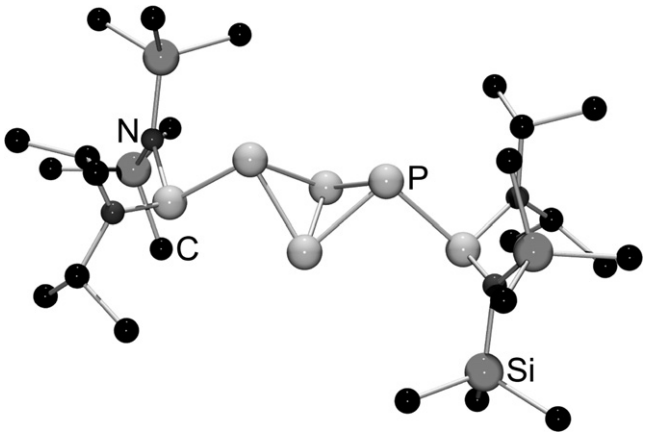

Fig. 6.1. Single crystal structure of the tetraphosphabicyclo[1.1.0]butane, $[(iPr_2N)(Me_3Si)_2NP]_2P_4$ [143]. Hydrogen atoms have been omitted for clarity.

toluene yielded the tetraphosphabicyclo[1.1.0]butane as shown in Scheme 6.3. Due to the unsymmetrical nature of the substituents on the diphosphine, the product was isolated and as a mixture of *meso*- and *rac*-diastereoisomers that cocrystallize (Fig. 6.1). The resulting structure indicates this species likely formed through steps 1 and 2 as listed above. The thermal stability imparted by the bulky phosphine substituents should be noted (i.e. preparation in refluxing toluene).

Most recently, Cossiart and Cummins [144] showed that a number of phosphines and polyphosphines could be prepared *via* a radical route through the use of a Ti(III) reagent, $Ti(N[tBu]Ar)_3$ ($Ar = 3,5\text{-}Me_2C_6H_3$), and various R–X species (R–X = PhBr, CyBr, Me_3SiI, Ph_3SnCl, Scheme 6.4). The titanium complex is used stoichiometrically to abstract X• (X = halide) to form the corresponding Ti(IV) complex and generate R•. The group 14 radicals then react with white phosphorus to form the tertiary phosphine. Depending on the stoichiometry, yields are 95% or higher for each substitutent. By modifying the stoichiometry tetraphenyldiphosphine, $Ph_2P–PPh_2$, can be isolated and is one of the intermediates in the fragmentation of white phosphorus by Ph• radicals. Using more sterically hindered substituents such as Mes or DMP results in the isolation of other plausible models of intermediates. Reaction of MesBr with the titanium reagent results in the formation of $(MesP)_3$ in a 61% isolated yield. Presumably, due to the mild reaction conditions and the lack of formation of $(MesP)_4$ [145], the mechanism may likely follow step 3a listed above. However, it cannot be ruled

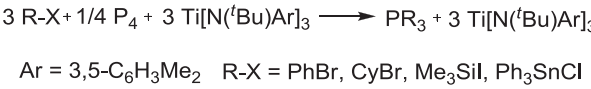

Scheme 6.4. Formation of tertiary phosphines *via* radicals formed using a Ti(III) reagent.

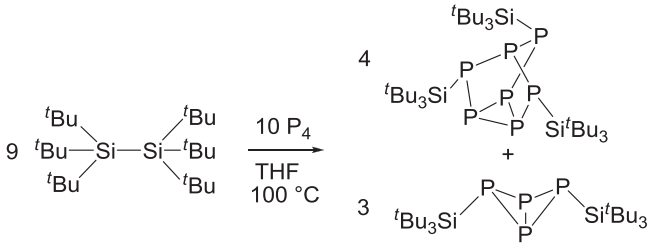

Scheme 6.5. Homolytic cleavage of the Si–Si bond of superdisilane forms a silyl radical that reacts with P_4 forming two products.

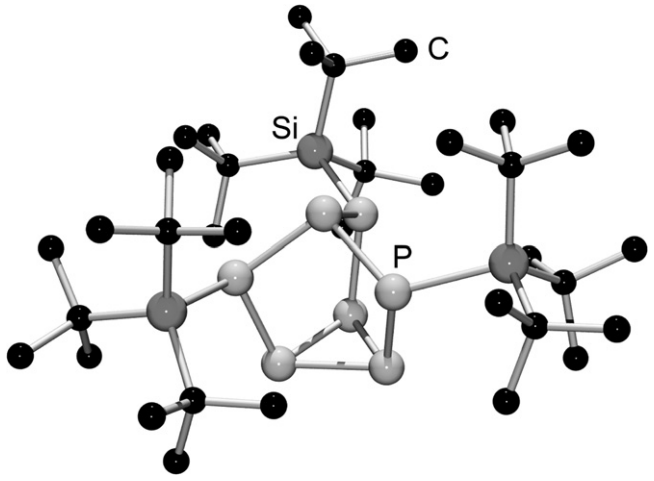

Fig. 6.2. Single crystal structure of tris(tri-*tert*-butylsilyl)heptaphosphanotricyclane [147]. Hydrogen atoms have been omitted for clarity.

out that $(MesP)_4$ is formed and due to steric strain is more reactive since the minor side product $Mes_2P–PMes_2$ could form from both the three- and four-membered species. Finally, using the sterically bulky DMP substituent, the *cis*,*trans*-DMP-P_4-DMP compound formed as the only product (78% isolated yield) when using DMP as the radical source.

The so-called superdisilane, $^tBu_3Si\text{-}Si^tBu_3$, readily forms the supersilyl radical, $^tBu_3Si^{\bullet}$, upon heating above 50 °C [146]. Thus, heating a mixture of superdisilane with white phosphorus at elevated temperatures gives a mixture of two products: the butterfly compound *trans*,*trans*-bis(tri-*tert*-butylsilyl)tetraphosphabicyclo[1.1.0]butane and the cage-type compound tris(tri-*tert*-butylsilyl)heptaphosphanotricyclane (Scheme 6.5) [147]. Clearly, the supersilyl radical reacts in the expected manner when forming the butterfly species, while the formation of the P_7 species is less obvious (Fig. 6.2).

7. Conclusion and outlook

Although the reaction of white phosphorus with *p*-block nucleophiles and electrophile initiated, ambiphilic centers is well on its way to being established, recent work by the Bertrand group has shown that there is much more to explore in the activation, fragmentation, aggregation and substitution using nucleophile initiated, ambiphilic centers such as singlet carbenes. Furthermore, radical-based chemistry involving white phosphorus appears to be underdeveloped and may prove fruitful based on recent success in the stoichiometric production of "normal" tertiary alkyl or aryl phosphines by Cossairt and Cummins [144]. Such innovation will continue to drive the resurgence of P_4 chemistry through the next decade. The catalytic derivatization of P_4 continues to be a challenge for phosphorus chemists. Of course, if catalysis can be achieved, another exciting chapter in phosphorus chemistry will begin.

Acknowledgements

The authors would like to thank Lauren Keyes for assistance in the preparation of the graphics related to the crystal structures including other members of the Masuda Research Group (Arthur Hendsbee, Tom Rogers, Sarah MacDonald) for obtaining many of the references in this review. J.D.M. thanks Saint Mary's University and the Natural Sciences and Engineering Research Council (Canada) Discovery Grant program for financial support. N.A.G. acknowledges the Office of the Dean of Science at Saint Mary's University for a Deans' Summer Research Award.

References

[1] F. Krafft, Angew. Chem. Int. Ed. Engl. 8 (1969) 660.
[2] M. Byko, JOM 59 (2007) 13.
[3] Derby City Council, 2010.
[4] I.S. Bell, H. Qian, P.A. Hamilton, P.B. Davies, J. Chem. Phys. 107 (1997) 8311.
[5] J. Emsley, The 13th Element: The Sordid Tale of Murder, Fire and Phosphorus, John Wiley & Sons, Inc., New York, 2000.
[6] W. Gleason, JOM 59 (2007) 17.
[7] O.J. Scherer, Angew. Chem. Int. Ed. Engl. 29 (1990) 1104.
[8] O.J. Scherer, Acc. Chem. Res. 32 (1999) 751.
[9] O.J. Scherer, Chem. Unserer Zeit. 34 (2000) 374.
[10] M. Ehses, A. Romerosa, M. Peruzzini, Top. Curr. Chem. 220 (2002) 107.
[11] M. Peruzzini, L. Gonsalvi, A. Romerosa, Chem. Soc. Rev. 34 (2005) 1038.
[12] M. Baudler, Angew. Chem. Int. Ed. Engl. 26 (1987) 419.
[13] M. Baudler, K. Glinka, Chem. Rev. 93 (1993) 1623.
[14] L. Maier, Fortschr. Chem. Forsch. 19 (1971) 1.
[15] C. Brown, R.F. Hudson, G.A. Wartew, Phosphorus Sulfur 5 (1978) 67.
[16] L. Riesel, Z. Chem. 19 (1979) 161.
[17] H.A. Lehmann, G. Grossmann, Pure Appl. Chem. 52 (1980) 905.
[18] V.A. Milyukov, Y.H. Budnikova, O.G. Sinyashin, Russ. Chem. Rev. 74 (2005) 781.
[19] Y.H. Budnikova, D.G. Yakhvarov, O.G. Sinyashin, J. Organomet. Chem. 690 (2005) 2416.
[20] Y.H. Budnikova, D.I. Tazeev, T.V. Gryaznova, O.G. Sinyashin, Russ. J. Electrochem. 42 (2006) 1127.
[21] Y.H. Budnikova, S.A. Krasnov, T.V. Graznova, A.P. Tomilov, V.V. Turigin, I.M. Magdeev, O.G. Sinyashin, Phosphorus, Sulfur Silicon Relat. Elem. 183 (2008) 513.
[22] E. Fluck, C.M.E. Pavlidou, R. Janoschek, Phosphorus Sulfur 6 (1979) 469.
[23] N.A. Piro, C.C. Cummins, J. Am. Chem. Soc. 131 (2009) 8764.
[24] R. Ahlrichs, S. Brode, C. Ehrhardt, J. Am. Chem. Soc. 107 (1985) 7260.
[25] M.K. Denk, A. Hezarkhani, Heteroatom Chem. 16 (2005) 453.
[26] N.A. Piro, C.C. Cummins, J. Am. Chem. Soc. 130 (2008) 9524.
[27] A.E. Douglas, K.S. Rao, Can. J. Phys. 36 (1958) 565.
[28] A. Pfitzner, Angew. Chem. Int. Ed. 45 (2006) 699.
[29] M. Haser, O. Treutler, J. Chem. Phys. 102 (1995) 3703.
[30] N.J. Brassington, H.G.M. Edwards, D.A. Long, J. Raman Spectrosc. 11 (1981) 346.
[31] L.R. Maxwell, S.B. Hendricks, V.M. Mosley, J. Chem. Phys. 3 (1935) 699.
[32] A. Simon, H. Borrmann, J. Horakh, Chem. Ber. 130 (1997) 1235.
[33] A. Simon, H. Borrmann, H. Craubner, Phosphorus Sulfur 30 (1987) 507.
[34] H. Okudera, R.E. Dinnebier, A. Simon, Z. Kristallogr. 220 (2005) 259.
[35] R.E. Douthwaite, M.L.H. Green, S.J. Heyes, M.J. Rosseinsky, J.F. Turner, J. Chem. Soc., Chem. Commun. (1994) 1367.
[36] P. Mal, B. Breiner, K. Rissanen, J.R. Nitschke, Science 324 (2009) 1697.
[37] B.M. Cossairt, C.C. Cummins, J. Am. Chem. Soc. 131 (2009) 15501.
[38] R. Hultgren, N.S. Gingrich, B.E. Warren, J. Chem. Phys. 3 (1935) 351.
[39] A. Brown, S. Rundqvist, Acta Crystallogr. 19 (1965) 684.
[40] J.C. Jamieson, Science 139 (1963) 1291.
[41] R. Ahuja, Phys. Status Solidi B 235 (2003) 282.
[42] T. Kikegawa, H. Iwasaki, Acta Crystallogr. B39 (1983) 158.
[43] S. Lange, P. Schmidt, T. Nilges, Inorg. Chem. 46 (2007) 4028.
[44] W.L. Roth, T.W. DeWitt, A.J. Smith, J. Am. Chem. Soc. 69 (1947) 2881.
[45] M. Rubenstein, F.M. Ryan, J. Electrochem. Soc. 113 (1966) 1063.
[46] A. Pfitzner, E. Freudenthaler, Angew. Chem. Int. Ed. Engl. 34 (1995) 1647.
[47] A. Pfitzner, M.F. Braeu, J. Zweck, G. Brunklaus, H. Eckert, Angew. Chem. Int. Ed. 43 (2004) 4228.
[48] H. Hartl, Angew. Chem. Int. Ed. Engl. 34 (1996) 2637.
[49] M. Ruck, D. Hoppe, B. Wahl, P. Simon, Y. Wang, G. Seifert, Angew. Chem. Int. Ed. 44 (2005) 7616.
[50] W. Hittorf, Ann. Phys. Chem. 126 (1865) 193.
[51] H. Thurn, H. Krebs, Angew. Chem. Int. Ed. Engl. 5 (1966) 1047.
[52] H. Thurn, H. Krebs, Acta Crystallogr. B25 (1969) 125.
[53] S. Boecker, M. Haeser, Z. Anorg. Allg. Chem. 621 (1995) 358.
[54] M.H. Moeller, W. Jeitschko, J. Solid State Chem. 65 (1986) 178.

[55] A. Pfitzner, E. Freudenthaler, Z. Naturforsch. B52 (1997) 199.
[56] R.A.L. Winchester, M. Whitby, M.S.P. Shaffer, Angew. Chem. Int. Ed. 48 (2009) 3616.
[57] B.A. Trofimov, S.F. Malysheva, N.K. Gusarova, N.A. Belogorlova, V.A. Kuimov, B.G. Sukhov, N.P. Tarasova, Y.V. Smetannikov, A.S. Vilesov, L.M. Sinegovskaya, K.Y. Arsent'ev, E.V. Likhoshvai, Dokl. Chem. 427 (2009) 153.
[58] V.G. Tsirelson, N.P. Tarasova, M.F. Bobrov, Y.V. Smetannikov, Heteroatom Chem. 17 (2006) 572.
[59] A. Hirsch, Z. Chen, H. Jiao, Angew. Chem. Int. Ed. 40 (2001) 2834.
[60] P.C. Hiberty, F. Volatron, Heteroatom Chem. 18 (2007) 129.
[61] S. Nagase, K. Ito, Chem. Phys. Lett. 126 (1986) 43.
[62] M.T. Nguyen, A.F. Hegarty, J. Chem. Soc., Chem. Commun. (1986) 383.
[63] P.v.R. Schleyer, H. Jiao, N.J.R. van Eikema Hommes, V.G. Malkin, O. Malkina, J. Am. Chem. Soc. 119 (1997) 12669.
[64] S. Sakai, J. Phys. Chem. A 106 (2002) 10370.
[65] J.J. Engelberts, R.W.A. Havenith, J.H. Van Lenthe, L.W. Jenneskens, P.W. Fowler, Inorg. Chem. 44 (2005) 5266.
[66] R. Janoschek, Chem. Ber. 122 (1989) 2121.
[67] D. Schroder, H. Schwarz, M. Wulf, H. Sievers, P. Jutzi, M. Reiher, Angew. Chem. Int. Ed. 38 (1999) 3513.
[68] B.M. Gimarc, D.S. Warren, Inorg. Chem. 32 (1993) 1850.
[69] M.W. Schmidt, M.S. Gordon, Inorg. Chem. 24 (1985) 4503.
[70] G. Trinquier, J.P. Daudey, N. Komiha, J. Am. Chem. Soc. 107 (1985) 7210.
[71] E.A. Halevi, H. Bock, B. Roth, Inorg. Chem. 23 (1984) 4376.
[72] R. Huang, H. Li, Z. Lin, S. Yang, J. Phys. Chem. 99 (1995) 1418.
[73] Z.Y. Liu, R.B. Huang, L.S. Zheng, Z. Phys. D38 (1996) 171.
[74] M.D. Chen, R.B. Huang, L.S. Zheng, Q.E. Zhang, C.T. Au, Chem. Phys. Lett. 325 (2000) 22.
[75] J.-N. Feng, M. Cui, X.-R. Huang, P. Otto, F.L. Gu, J. Mol. Struct. 425 (1998) 201.
[76] G. Seifert, R.O. Jones, J. Chem. Phys. 96 (1992) 2951.
[77] R.O. Jones, G. Seifert, J. Chem. Phys. 96 (1992) 7564.
[78] R.O. Jones, G. Gantefoer, S. Hunsicker, P. Pieperhoff, J. Chem. Phys. 103 (1995) 9549.
[79] R. Huang, H. Li, Z. Lin, S. Yang, Surf. Rev. Lett. 3 (1996) 167.
[80] R. Janoschek, Chem. Ber. 125 (1992) 2687.
[81] J. Bai, E. Leiner, M. Scheer, Angew. Chem. Int. Ed. 41 (2002) 783.
[82] M. Scheer, L. Gregoriades, J. Bai, M. Sierka, G. Brunklaus, H. Eckert, Chem. Eur. J. 11 (2005) 2163.
[83] F. Dielmann, R. Merkle, S. Heinl, M. Scheer, Z. Naturforsch. B64 (2009) 3.
[84] O.J. Scherer, H. Sitzmann, G. Wolmershaeuser, J. Organomet. Chem. 268 (1984) C9.
[85] O.J. Scherer, Comments Inorg. Chem. 6 (1987) 1.
[86] O.J. Scherer, J. Schwalb, H. Swarowsky, G. Wolmershaeuser, W. Kaim, R. Gross, Chem. Ber. 121 (1988) 443.
[87] N.C. Baird, Can. J. Chem. 62 (1984) 341.
[88] R.O. Jones, D. Hohl, J. Chem. Phys. 92 (1990) 6710.
[89] P. Ballone, R.O. Jones, J. Chem. Phys. 100 (1994) 4941.
[90] G. Trinquier, J.P. Malrieu, J.P. Daudey, Chem. Phys. Lett. 80 (1981) 552.
[91] M. Haeser, U. Schneider, R. Ahlrichs, J. Am. Chem. Soc. 114 (1992) 9551.
[92] A.J. Karttunen, M. Linnolahti, T.A. Pakkanen, Chem. Eur. J. 13 (2007) 5232.
[93] M.M. Rauhut, A.M. Semsel, J. Org. Chem. 28 (1963) 471.
[94] M.M. Rauhut, A.M. Semsel, J. Org. Chem. 28 (1963) 473.
[95] B.A. Trofimov, L. Brandsma, S.N. Arbuzova, N.K. Gusarova, Russ. Chem. Bull. 46 (1997) 849.
[96] A. Schmidpeter, G. Burget, F. Zwaschka, W.S. Sheldrick, Z. Anorg. Allg. Chem. 527 (1985) 17.
[97] R. Riedel, H.D. Hausen, E. Fluck, Angew. Chem. 97 (1985) 1050.
[98] A.R. Fox, R.J. Wright, E. Rivard, P.P. Power, Angew. Chem. Int. Ed. 44 (2005) 7729.
[99] W.T.K. Chan, F. Garcia, A.D. Hopkins, L.C. Martin, M. McPartlin, D.S. Wright, Angew. Chem. Int. Ed. 46 (2007) 3084.
[100] A. Lorbach, A. Nadj, S. Tuellmann, F. Dornhaus, F. Schoedel, I. Saenger, G. Margraf, J.W. Bats, M. Bolte, M.C. Holthausen, M. Wagner, H. Lerner, Inorg. Chem. 48 (2009) 1005.
[101] N. Wiberg, A. Woerner, K. Karaghiosoff, D. Fenske, Chem. Ber. 130 (1997) 135.
[102] H. Lerner, M. Bolte, K. Karaghiosoff, M. Wagner, Organometallics 23 (2004) 6073.
[103] H. Lerner, M. Wagner, M. Bolte, Chem. Commun. (2003) 990.
[104] H. Lerner, G. Margraf, L. Kaufmann, J.W. Bats, M. Bolte, M. Wagner, Eur. J. Inorg. Chem. (2005) 1932.
[105] A. Schmidpeter, S. Lochschmidt, G. Burget, W.S. Sheldrick, Phosphorus Sulfur 18 (1983) 23.
[106] A. Schmidpeter, G. Burget, W.S. Sheldrick, Chem. Ber. 118 (1985) 3849.
[107] A. Schmidpeter, G. Burget, Phosphorus Sulfur 22 (1985) 323.
[108] A. Schmidpeter, G. Burget, H.G. Von Schnering, D. Weber, Angew. Chem. Int. Ed. Engl. 23 (1984) 816.
[109] C. Rotter, M. Schuster, K. Karaghiosoff, Inorg. Chem. 48 (2009) 7531.
[110] E.K. Badeeva, E.S. Batyeva, A.T. Gubaidullin, I.A. Litvinov, O.G. Sinyashin, Russ. J. Gen. Chem. 75 (2005) 835.
[111] M.B. Power, A.R. Barron, Angew. Chem. Int. Ed. Engl. 30 (1991) 1353.
[112] W.W. Schoeller, Phys. Chem. Chem. Phys. 11 (2009) 5273.
[113] H.M. Tuononen, R. Roesler, J.L. Dutton, P.J. Ragogna, Inorg. Chem. 46 (2007) 10693.
[114] W.W. Schoeller, V. Staemmler, P. Rademacher, E. Niecke, Inorg. Chem. 25 (1986) 4382.
[115] R. Damrauer, S.E. Pusede, Organometallics 28 (2009) 1289.
[116] R. Damrauer, S.E. Pusede, G.M. Staton, Organometallics 27 (2008) 3399.
[117] K. Nyiri, T. Szilvasi, T. Veszpremi, Dalton Trans. 39 (2010) 9347.
[118] J.D. Masuda, W.W. Schoeller, B. Donnadieu, G. Bertrand, Angew. Chem. Int. Ed. 46 (2007) 7052.
[119] J.D. Masuda, W.W. Schoeller, B. Donnadieu, G. Bertrand, J. Am. Chem. Soc. 129 (2007) 14180.
[120] O. Back, G. Kuchenbeiser, B. Donnadieu, G. Bertrand, Angew. Chem. Int. Ed. 48 (2009) 5530.
[121] C. Dohmeier, C. Robl, M. Tacke, H. Schnoeckel, Angew. Chem. Int. Ed. 30 (1991) 564.
[122] J. Gauss, U. Schneider, R. Ahlrichs, C. Dohmeier, H. Schnoeckel, J. Am. Chem. Soc. 115 (1993) 2402.
[123] C. Dohmeier, H. Schnoeckel, C. Robl, U. Schneider, R. Ahlrichs, Angew. Chem. Int. Ed. 33 (1994) 199.
[124] Y. Peng, H. Fan, H. Zhu, H.W. Roesky, J. Magull, C.E. Hughes, Angew. Chem. Int. Ed. 43 (2004) 3443.
[125] G. Prabusankar, A. Doddi, C. Gemel, M. Winter, R.A. Fischer, Inorg. Chem. 49 (2010) 7976.
[126] W. Uhl, W. Hiller, M. Layh, W. Schwarz, Angew. Chem. Int. Ed. 31 (1992) 1364.
[127] W. Uhl, M. Benter, Chem. Commun. (1999) 771.
[128] M. Driess, A.D. Fanta, D. Powell, R. West, Angew. Chem. Int. Ed. 28 (1989) 1038.
[129] A.D. Fanta, R.P. Tan, N.M. Comerlato, M. Driess, D.R. Powell, R. West, Inorg. Chim. Acta 198–200 (1992) 733.
[130] M. Driess, H. Pritzkow, M. Reisgys, Chem. Ber. 124 (1991) 1923.
[131] Y. Xiong, S. Yao, E. Bill, M. Driess, Inorg. Chem. 48 (2009) 7522.
[132] Y. Xiong, S. Yao, M. Brym, M. Driess, Angew. Chem. Int. Ed. 46 (2007) 4511.
[133] I. Krossing, I. Raabe, Angew. Chem. Int. Ed. 40 (2001) 4406.
[134] M. Gonsior, I. Krossing, L. Muller, I. Raabe, M. Jansen, L. Van Wullen, Chem. Eur. J. 8 (2002) 4475.
[135] J.J. Weigand, M. Holthausen, R. Frohlich, Angew. Chem. Int. Ed. 48 (2009) 295.
[136] M.H. Holthausen, J.J. Weigand, J. Am. Chem. Soc. 131 (2009) 14210.
[137] D. Bourissou, O. Guerret, F.P. Gabbai, G. Bertrand, Chem. Rev. 100 (2000) 39.
[138] G.D. Frey, V. Lavallo, B. Donnadieu, W.W. Schoeller, G. Bertrand, Science 316 (2007) 439.
[139] V. Lavallo, J. Mafhouz, Y. Canac, B. Donnadieu, W.W. Schoeller, G. Bertrand, J. Am. Chem. Soc. 126 (2004) 8670.
[140] V. Lavallo, Y. Canac, B. Donnadieu, W.W. Schoeller, G. Bertrand, Angew. Chem. Int. Ed. 45 (2006) 3488.
[141] V. Lavallo, Y. Canac, B. Donnadieu, W.W. Schoeller, G. Bertrand, Science 312 (2006) 722.
[142] B.W. Tattershall, N.L. Kendall, Polyhedron 13 (1994) 1517.
[143] J. Bezombes, P.B. Hitchcock, M.F. Lappert, J.E. Nycz, Dalton Trans. (2004) 499.
[144] B.M. Cossairt, C.C. Cummins, New J. Chem. 34 (2010) 1533.
[145] C. Couret, J. Escudie, H. Ranaivonjatovo, J. Satge, Organometallics 5 (1986) 113.
[146] N. Wiberg, Coord. Chem. Rev. 163 (1997) 217.
[147] I. Kovacs, G. Baum, G. Fritz, D. Fenske, N. Wiberg, H. Schuster, Karaghiosoff, Z. Anorg. Allg. Chem. 619 (1993) 453.
[148] B.M. Cossairt, N.A. Piro, C.C. Cummins, Chem. Rev. 110 (2010) 4164.
[149] M. Caporali, L. Gonsalvi, A. Rossin, M. Peruzzini, Chem. Rev. 110 (2010) 4178.
[150] M. Scheer, G. Balazs, A. Seitz, Chem. Rev. 110 (2010) 4236.